

Cool Young Stars in the Northern Hemisphere: β Pictoris and AB Doradus Moving Group Candidates

Joshua E. Schlieder^{1,2,3}, Sébastien Lépine⁴, and Michal Simon^{1,3}

(Accepted to the Astronomical Journal)

ABSTRACT

As part of our continuing effort to identify new, low-mass members of nearby, young moving groups (*NYMGs*), we present a list of young, low-mass candidates in the northern hemisphere. We used our proven proper motion selection procedure and *ROSAT*-X-ray and *GALEX*-UV activity indicators to identify 204 young stars as candidate members of the β Pictoris and AB Doradus *NYMGs*. Definitive membership assignment of a given candidate will require a measurement of its radial velocity and distance. We present a simple system of indices to characterize the young candidates and help prioritize follow up observations. New group members identified in this candidate list will be high priority targets for: 1) exoplanet direct imaging searches, 2) the study of post-T-Tauri astrophysics, 3) understanding recent local star formation, and 4) the study of local galactic kinematics. Information available now allows us to identify 8 likely new members in the list. Two of these, a late-K and an early-M dwarf, we find to be likely members of the β Pic group. The other six stars are likely members of the AB Dor moving group. These include an M dwarf triple system, and three very cool objects that may be young brown dwarfs, making them the lowest-mass, isolated objects proposed in the AB Dor moving group to date.

Subject headings: open clusters and associations: individual (β Pictoris moving group, AB Doradus moving group) – stars: pre-main-sequence – stars: kinematics

¹Department of Physics and Astronomy, Stony Brook University, Stony Brook, NY 11794, michal.simon@stonybrook.edu

²Currently at Max-Planck-Institut für Astronomie, Königstuhl 17, 69117 Heidelberg, Germany, schlieder@mpia-hd.mpg.de

³Visiting Astronomer, NASA Infrared Telescope Facility (IRTF).

⁴Department of Astrophysics, American Museum of Natural History, Central Park West at 79th Street, New York, NY 10024, lepine@amnh.org

1. Introduction

Well characterized samples of low-mass, pre-main sequence (*PMS*) stars are important for understanding star formation and evolution, the circumstellar environment, and planetary system formation. These stars are attractive targets for exoplanet searches by direct imaging because young, massive planets are expected to be self-luminous from gravitational contraction and the contrast between host star and planet is more favorable when the star is intrinsically faint. The nearest and youngest stars in clusters lie in the Taurus and Ophiuchus star forming regions (*SFRs*) with ages $\sim 1 - 5$ Myr and distances 120 - 145 pc. Their distances limit the detail with which they can be studied. Nearby, low-mass *PMS* stars that are no longer associated with their *SFRs* have long been sought following Herbig’s (1978) suggestion that they may exist in large numbers mingled with field stars. Post-T-Tauri stars (*PTTS*), with ages $\sim 10^7 - \sim 10^8$ yr, exhibit properties associated with stellar youth, such as chromospheric activity, lithium absorption, and rapid rotation, which provide the means to distinguish them among older field stars.

Stellar counterparts to *ROSAT* (Voges et al. 1999, 2000; hereafter V99, V00) X-ray sources and the compilation of precision astrometric catalogs (e.g. the *Hipparcos* catalog, Perryman et al. 1997) have yielded the identification of nearby, young stars as members of coeval groups characterized by the common motion of their members through the Galaxy. These groups of stars are known as nearby, young moving groups (*NYMGs*) (see Zuckerman & Song 2004, hereafter ZS04; Torres et al. 2008, hereafter T08). Members of *NYMGs* have ages < 100 Myr and lie at distances $\lesssim 100$ pc (T08). The ages, space motions, and sky distributions of stars in the *NYMGs* suggest that they share a common origin. Kinematic traceback studies show they may be related to a star formation event in the Sco-Cen region (Mamajek & Feigelson 2001, Fernández et al. 2008).

Most members of the known moving groups are concentrated in the south. However, we began our search for new, low-mass *NYMG* members in the β Pictoris moving group (*BPMG*, Lépine & Simon 2009, hereafter LS09) and expanded it to the AB Doradus moving group (*ABDMG*, Schlieder et al. 2010, hereafter S10) because they have known members in the north. The northern hemisphere presents a relatively untapped resource in the search for moving group members.

To date, confirmed members of the *BPMG* and *ABDMG* show a marked deficiency in low-mass stars between spectral subtypes M0 to M6. If those moving groups have a mass function consistent with field stars (see Bochanski et al. 2010), then astronomers are currently missing the bulk of the β Pic and AB Dor members. There are two primary factors contributing to the observed deficiency of known low-mass members: 1) low-mass stars are intrinsically faint, thus the majority are beyond the magnitude limits of the *Hipparcos* and

Tycho-2 astrometric catalogs which, along with the *ROSAT* catalogs, have so far been used as the primary sources for identifying new group members. 2) The lowest-mass stars lack reliable youth diagnostics from which the missing stars could be easily identified. Traditional activity indicators, X-ray and $H\alpha$ emission, are increasingly less reliable for spectral types (*SpTy*) later than M4 because most older, field stars are active in that spectral range (West et al. 2008, 2011, hereafter W11). This is probably a consequence of the transition to fully convective interiors. Lithium is also depleted for most low-mass stars at the ages of the *NYMGs* (Palla & Randich 2004) which makes the detection/non-detection of the Li 6708 Å line an unreliable indicator of age. Furthermore, Baraffe and Chabrier (2010, hereafter BC10) have also shown that Li depletion may be strongly affected by stellar accretion history in low-mass stars.

LS09 developed an astrometric technique to identify low-mass candidates of *NYMGs* in proper motion catalogs. The projected mean motion vector of a known moving group is used to identify candidates based on their proper motion and optical/IR photometry. The visual magnitude of the proper motion samples to which LS09 applied this technique ($V < 12$) limited the identification of likely new members to stars earlier than approximately M2 *SpTy* (LS09). S10 expanded the technique to a preliminary version of the deeper ($V < 19$) *SUPERBLINK* catalog (*SBK*, Lépine et al. 2012, in prep.) to probe into the mid-M range.

Several other efforts are underway to identify low-mass *NYMG* members. Shkolnik et al. (2009, hereafter Sh09) use *ROSAT* X-ray data and spectroscopic follow up to identify nearly 150 nearby, young M dwarfs in a $d < 25$ pc sample, at least some of which are likely to be *NYMG* members. Shkolnik et al. (2011, hereafter Sh11) present an analysis of M dwarfs in the *HST* Guide Star Catalogue (Lasker et al. 2008) and the *2MASS* All-Sky Catalog of Point Sources (*2MASS*, Skrutskie et al. 2006) having *GALEX* counterparts to calibrate UV emission as a youth indicator in low-mass stars. UV emission was then used as a basis to identify two new members of the ~ 10 Myr old TW Hydrae association. Kiss et al. (2011) use a selection technique similar to T08 and data from The Radial Velocity Experiment (*RAVE*, Steinmetz et al. 2006) to identify new *NYMG* members in the south. Rice et al. (2010) report the first isolated brown dwarf member of the *BPMG* as a result of a large scale astrometric and spectroscopic survey of brown dwarfs. Others have started to use *GALEX* data to identify cool young stars as well, focusing on UV excess as a diagnostic (Findeisen & Hillenbrand 2010, hereafter FH10; Rodriguez et al. 2011, hereafter R11). A program is also underway that uses a selection technique very similar to LS09, S10, and this work but assigns membership probabilities to candidates using Bayesian analysis techniques. This search focuses on β Pic, AB Dor, and Tuc/Hor candidates (see Rice et al. 2011).

In §2 and §3 of this paper we apply the techniques described in LS09 and S10 to search for

BPMG and *ABDMG* candidates in the *Tycho-2* catalog (Høg et al. 2000, hereafter H00), the *LSPM-North* catalog (Lépine and Shara 2005, hereafter LS05), and the now complete northern hemisphere *SBK* catalog. This extension permits identification of moving group candidates with *SpTy*’s beyond M4, which raises the problem of identifying the young stars among them. For mid-M dwarfs and later, the gravity sensitive alkali lines, such as the neutral sodium lines (*NaI*), can serve as proxies for youth. At a few tens of Myrs age, these stars are still contracting to the main sequence (*MS*) and have lower photospheric gravities than they will have later; this makes the *NaI* doublet at ~ 8200 Å a useful indicator of age in low-mass stars (Schlieder et al. 2011). The extensive spectroscopic observations required to study this feature are however beyond the scope of this paper. We therefore describe in §4 our list of young β Pic and AB Dor candidates in the north identified using our selection technique and the X-ray/UV youth criteria described in Sh09 and Sh11. We also carry out a preliminary study of the candidates to determine those for which these youth indicators are most reliable. In §5 we investigate the bulk properties of the sample to guide follow up priority. In §6 we describe likely new members identified in the analysis presented and we summarize our results in §7.

2. Candidate Selection

T08 lists 50 *BPMG* members with membership probability $\geq 90\%$ for all but 3 stars¹. The membership probabilities were calculated using the full, six-dimensional galactic kinematics of the group in a *k*-NN model (T08). We include all 50 known members in our analysis. The known *BPMG* members lie at a median distance of ~ 35 pc and have ages 10-20 Myr (T08). The motion of the group through the galaxy is defined using *U*, *V*, and *W* space velocities (Johnson and Soderblom 1987) with means (U_{BPMG} , V_{BPMG} , W_{BPMG}) = $(-10.1 \pm 2.1, -15.9 \pm 0.8, -9.2 \pm 1.0)$ km s⁻¹ relative to the Sun (T08). In this coordinate system, *U* is positive toward the galactic center, *V* is positive in the direction of solar motion around the Galaxy, and *W* is positive toward the north galactic pole. The group shows extension in the direction toward the galactic center (Fig. 1), a feature common to all *NYMGs* younger than 30 Myr (T08)².

The 89 known members of the *ABDMG* lie at a median distance of ~ 30 pc and have ages of ~ 70 Myr (T08). All of these stars have a membership probability in T08 $\geq 85\%$. The

¹Proposed *BPMG* members HD 203, HD 15115, and HD 199143 have probabilities 75%, 60%, and 75% respectively

²*XYZ* distances are defined positive in the same directions as *UVW* velocities.

mean velocities of AB Dor group members are $(U_{ABDMG}, V_{ABDMG}, W_{ABDMG}) = (-6.8 \pm 1.3, -27.2 \pm 1.2, -13.3 \pm 1.6)$ km s⁻¹. These space velocities are comparable to those of Pleiades open cluster members. Luhman et al. (2005) and Ortega et al. (2007) argue that the *ABDMG* may be remnant of the star formation event that formed the Pleiades. Possibly coincidentally, the space velocities of some AB Dor stars are similar to β Pic stars in the *U* and *W* plane. The group lacks the *X* direction extension of younger *NYMGs* and exhibits a more uniform galactic distance distribution (see Fig. 2).

LS09 and S10 have described the proper motion selection algorithm in detail. To produce a list of young candidates in the northern hemisphere we performed only the first 3 steps in the search procedure: 1) isolate a sample of stars in a proper motion catalog whose proper motion vectors are consistent with moving group membership (see LS09 Eqns. (1-4)), 2) identify stars in that subsample whose photometric distance (d_{phot}) is consistent with the kinematic distance (d_{kin}), which is derived from the proper motion assuming group membership (see LS09 Eqns. (5-7)), 3) trim this sample to include only stars exhibiting indicators of youth. After this, all that will be required is a confirmation that the radial velocity (*RV*) and astrometric distance are consistent with *NYMG* membership. This follow up work is now in the planning stages. We follow the labeling convention introduced in S10:

1. *Candidate* - A low-mass star having proper motion and photometry consistent with *NYMG* membership
2. *Probable Young Candidate (PYC)* - A candidate exhibiting indicators of youth
3. *Likely New Member (LNM)* - A *PYC* having a *RV* or distance consistent with *NYMG* membership

Because the search parameters govern the candidates selected, we describe the parameters in detail and define the limits used in this search:

Lower Proper Motion Limit, μ_{min} : A lower limit that is very small will introduce contamination from field stars whose proper motions align with the projected mean motion of the group by chance. We chose $\mu_{min} = 40$ mas yr⁻¹ as a lower limit because the majority of known *BPMG* and *ABDMG* members have $40 \text{ mas yr}^{-1} \leq \mu \leq 200 \text{ mas yr}^{-1}$ (see Fig. 3).

Dispersion About Average Space Motion, ϕ : The scalar product of the mean projected motion of the group with the proper motion of a catalog star, calculated in the plane of the sky local to the star, defines $\cos\phi$ (LS09, Eqn. 3). Stars that are actual *NYMG* members will have ϕ close to 0. The largest acceptable value of ϕ , called ϕ_{max} , depends on the *UVW* velocity dispersion of known moving group members and can be assessed by calculating ϕ for each

known member (see Fig. 4). We choose $\phi_{max} = 10^\circ$ because it includes most of the known *BPMG* and *ABDMG* members and limits contamination from kinematic interlopers.

Kinematic Distance, d_{kin} : If one assumes that a candidate selected by its proper motion actually belongs to the moving group considered, then its d_{kin} can be calculated from the magnitude of the proper vector (LS09, Eqn. 6) and used as a selection parameter in two ways. First, a comparison of candidate and known member d_{kin} can act as a selection cut. The range of d_{kin} accepted when searching for candidates of an *NYMG* is again determined from the distribution of known members (Fig. 5). Both d_{kin} distributions peak between 30-40 pc with an upturn at 70 pc. Three of the 5 stars in the 70-80 pc range in the *BPMG* are later than *SpTy* K4, and only one has a measured parallax. The upturn at 70 pc in the *ABDMG* is more drastic, with more than 3 times the stars in the previous bin. All 15 of the proposed *ABDMG* members in the 70-80 pc bin are earlier than mid-K type. However, only 2 have measured parallaxes. Since most of the stars in the 70-80 pc bins and beyond do not have measured distances we conservatively choose $d_{kin} \leq 70$ pc as the cutoff in the candidate search.

Second, the d_{kin} is used to calculate a pseudo-absolute K magnitude (M_k) in an M_k vs. ($V-K_s$) color-magnitude diagram (*CMD*). Candidates that are true *NYMG* members will be positionally and photometrically consistent with the cluster sequence of known group members in the *CMD* (see Fig. 6). Any candidate remaining in the sample after previous cuts that falls outside of the cluster-sequence locus is presumed to have its true distance over or under-estimated by d_{kin} and is rejected from the sample.

(V- K_s) Color: A lower limit on the ($V-K_s$) color determines the upper bound on the mass of the candidates. A $0.7 M_\odot$ dwarf with an age of 40 Myr will be *SpTy* \sim K7 and have ($V-K_s$) ≈ 3.2 (Siess et al. 2000, hereafter SDF2000). We used this value to concentrate our search on M dwarf candidates and avoid a high level of giant contamination (see Fig. 6).

Proper motion catalogs are magnitude and proper motion limited. Thus, searching several catalogs with complementary limits allows for the identification of all candidates within the combined limits of the search parameters and catalogs. The combined properties of the catalog subsamples we searched for northern hemisphere candidates are $\delta \geq 0^\circ$, $\mu \geq 40$ mas yr $^{-1}$, and complete to $V = 19$ mag. The individual catalogs we searched are as follows:

The Tycho-2 catalog contains positions, proper motions, and photometric data for ~ 2.5 million stars. The catalog is $\sim 99\%$ complete to $V \approx 11.0$, with a limiting magnitude of $V \approx 13.0$, and has proper motion accuracy of 2.5 mas yr $^{-1}$ (H00). We selected a subsample of northern hemisphere *Tycho-2* stars with $\mu \geq 40$ mas yr $^{-1}$ ($\sim 120,000$ stars) which is cross

correlated with *2MASS* to obtain near-IR J , H , and K_s magnitudes. Our previous results show that searches in the *Tycho-2* catalog return candidates that are mostly earlier than $SpTy \sim M3$ (S10), a result of the V magnitude limit of the catalog.

The *LSPM-North* catalog is an astrometric catalog of positions, proper motions, and multi-band photometry of $\sim 62,000$ high proper motion stars produced by data mining the Digitized Sky Surveys using specially developed software (LS05). The catalog contains stars with $\mu > 150 \text{ mas yr}^{-1}$ ($\mu_{err} \approx 8 \text{ mas yr}^{-1}$) north of the celestial equator and is $\sim 99\%$ complete for $12.0 < V < 19.0$ with a faint limit of $V = 21.0$ (LS05). *LSPM-North* complements the magnitude range of *Tycho-2*, overlapping it in some cases, and allows access to *NYMG* candidates down to $\sim 0.1 M_\odot$.

SUPERBLINK (*SBK*) is the smaller proper motion ($40 \text{ mas yr}^{-1} \leq \mu \leq 150 \text{ mas yr}^{-1}$) counterpart of the *LSPM-North* catalog and was produced using the same technique and thus retains the same limits (Sébastien Lépine, private communication). This database contains ~ 1.5 million stars with $\delta > 0^\circ$. The lower proper motion limit of *SBK* allows access to a larger spatial volume and hence more potential *NYMG* candidates unavailable in the *Tycho-2* or *LSPM-North* catalogs.

3. β Pic and AB Dor Group Candidates

We apply the search algorithm to the proper motion catalogs using the search parameter limits discussed in §2 to identify candidates of the *BPMG* and *ABDMG*. We emphasize that our technique is statistical in nature; it can identify candidates only within the limits chosen to characterize a group. The resulting list of candidates includes recovered known members, stars previously investigated in this project (LS09, S10), contaminants, and many new *NYMG* candidates, some of which will eventually become *LNMs*. We describe here the subsamples in the initial candidate list before presenting the final young sample.

The search for *BPMG* candidates returns 132 stars (see Fig. 6). Only 2 previously known *BPMG* members are recovered (Table 1). We expected to recover 4 members based on their declinations and colors. The 2 not recovered, BD+30 397B and HIP 23418, are missing from the catalogs searched and fall outside of the *BPMG* sequence locus defined in Fig. 6 respectively. The remaining known *BPMG* members in T08 are not recovered because they lie in the southern hemisphere or have $(V-K_s)$ colors that are too blue. Nineteen of the candidates were already investigated (LS09, S10), we therefore delete these from the present list, leaving 111 *BPMG* candidates.

The search for *ABDMG* candidates identifies 582 stars. Compared to the *BPMG* this

is a much larger number of candidates and is a consequence of the older age of the *ABDMG*. For a given *SpTy*, a member of the *ABDMG* is fainter than one in the *BPMG*, thus the cluster sequence of the *ABDMG* lies lower in the *CMD* and the search algorithm picks up more contaminants (see Fig. 6). The candidate search recovered 4 known *ABDMG* members (Table 1). The declinations and colors of known *ABDMG* members allow for the recovery of 6 in the search. The 2 not recovered are HD 21845B, a close companion lacking sufficient photometric data in the catalogs, and BD+01 2447, which lies outside of the *ABDMG* sequence locus defined in Fig. 6. S10’s search included 9 of the candidates, we remove them from the sample leaving 569 *ABDMG* candidates.

After removal of known members and previously investigated stars, the candidate searches in the *BPMG* and *ABDMG* result in a sample of 680 low-mass moving group candidates. These remaining stars represent a mixture of different populations including old and young dwarfs and evolved stars such as late type giants. We may identify some of the interlopers by considering their locations in an $((J-H)$ vs. $(H-K_s))$ color-color diagram. Figure 7 shows the candidate diagram. We overplotted the expected sequences for A0 to M6 dwarfs and K to M giants (Bessel & Brett 1988; Bessell 1991). Nearly all of the candidates occupy the region expected for late-type dwarfs. A few fall outside of this region; 2 align with the expected giant sequence at $(J-H) \sim 0.8$ and fewer than 10 are coincident with the expected sequence for earlier dwarfs ($(J-H) \lesssim 0.55$ and $(H-K_s) \approx 0.1$). These candidates are not included in further analyses. The 7 candidates in the solid black box have colors representative of ultracool objects at the hydrogen burning limit. They are considered separately in §6. The remaining candidates must be screened for indicators of youth. We follow the procedures outlined in Sh09 and Sh11 and perform a very similar analysis of X-ray and UV flux to identify *PYC*s.

4. Probable Young Candidates

4.1. X-ray Analysis

We perform a positional cross-correlation of known (T08) and new (LS09, S10) late-type β Pic and AB Dor members and our candidate sample with the *ROSAT* All-Sky Survey Bright Source and Faint Source catalogs (*RASS-BSC* and *RASS-FSC*; V99, V00). All known late-type β Pic and AB Dor members and 147 candidates have *ROSAT* counterparts within $50''$. If a candidate had a counterpart outside of $25''$ they were individually checked for crowded fields and unreliable matches were removed. X-ray fluxes (F_X) were calculated from count rates and hardness ratios (Schmitt et al. 1995). Figure 8 shows $\log(F_X/F_{K_s})$ as a function of $(V-K_s)$ color for the previously mentioned subsamples. We choose to take

the ratio F_X/F_{K_s} to be consistent with the use of K_s throughout our analysis, and because F_{K_s} varies little with activity. We compare to Sh09, who takes the flux ratio using F_J , and see an average difference of ~ 0.1 dex between known *NYMG* member data points. This reflects the difference in J and K_s band magnitudes, we thus choose $\log(F_X/F_{K_s}) \geq -2.6$ as the cut for *PYC*s to be consistent with Sh09’s youth cut and the observed flux ratio difference. This choice includes $\sim 90\%$ of the known late-type *NYMG* members. We identify 114 *PYC*s having F_X/F_{K_s} comparable to or larger than known late-type *NYMG* members. The remaining 33 candidates that fall below the cut are removed from the sample. However, the strong X-ray flux detected in some of these *PYC*s may be unreliable as a youth indicator since they are later than mid-M; these stars will be discussed later in this section.

The dashed grey line in Fig. 8 represents a *ROSAT* All-Sky Survey detection limit for the candidate sample. The detection limit was estimated using the limiting count-rate in the *RASS-BSC* scaled to the source photon limit of the *RASS-FSC*³. This limiting count-rate was combined with an average sample exposure time of ~ 500 s, the average X-ray hardness ratio (*HR1*) of the known *NYMG* members, and model derived magnitudes from SDF2000 evolutionary models for 40 Myr late-K to mid-M dwarfs at 40 pc to generate the curve.

4.2. UV analysis

The NASA Galaxy Evolution Explorer (*GALEX*) is a space based 0.5m UV telescope sensitive to $1350 \text{ \AA} \leq \lambda \leq 2750 \text{ \AA}$ (Martin et al. 2005). Part of the mission is to produce an All-Sky Imaging Survey (*AIS*) in two bands: the near-UV (*NUV*, 1750 - 2750 \AA) and far-UV (*FUV*, 1350 - 1750 \AA). Sh11 showed that *GALEX NUV* and *FUV* data can be used to effectively identify young M-dwarfs beyond 100 pc, far surpassing the sensitivity of *ROSAT* and providing a new resource in the search for cool, young stars in the solar neighborhood (see also FH10 and R11).

We used *GalexView*⁴ to cross-correlate the known late-type *NYMG* subsample and our candidate list with the sixth data release of the *GALEX AIS*, which covers $\sim 75\%$ of the sky. We obtained *NUV* and *FUV* data when available for stars with counterparts within $5''$, the resolution of *GALEX FUV* channel. All known *NYMG* members are detected in *NUV* and

³The *RASS-BSC* limit is 0.05 cts s^{-1} in the 0.1-2.4 keV energy band, or ≥ 15 source photons in the exposure time. For the *RASS-FSC* the detection limit is ≥ 6 source photons in the exposure time.

⁴a webtool for accessing *GALEX* data available at <http://galex.stsci.edu/galexview/>

all except one are detected in FUV ⁵. Three hundred eighty nine candidates have a detection in at least one *GALEX* band.

Fig. 9 shows $\log(F_{NUV}/F_{K_s})$ as a function of $(V-K_s)$ for the 304 *NUV* active candidates and known group members. Comparing to Sh11 we see the same ~ 0.1 dex difference between our UV/K_s flux ratios and their UV/J ratios as in the X-ray analysis. We thus choose $\log(F_{NUV}/F_{K_s}) \geq -4.1$ and $\log(F_{FUV}/F_{K_s}) \geq -5.1$ as our cuts for *PYC*s, again to be consistent with Sh11 and include the flux difference between J and K_s bands. We identify 149 *PYC*s with strong *NUV* flux. Many candidates with strong *NUV* flux also have strong X-ray flux. There are 14 *PYC*s with both *NUV* and *FUV* flux and no *ROSAT* detection that would have been missed if *GALEX* data were unavailable. Candidates having a *GALEX NUV* detection in Fig. 9 but falling below the *PYC* cut are removed from the sample.

The estimated detection limit of the *GALEX AIS* is shown as the gray dashed line in Fig. 9. The limit was estimated using the *GALEX AIS* 5σ limiting *NUV* magnitude for a 100s exposure (Morrissey et al. 2005) and the same SDF2000 models as the X-ray limit. Some candidates that we consider *PYC*s due to strong *UV* emission fall below the curve. This can be attributed to two factors: 1) the exposure time, many of the candidates have actual exposure times >100 s, 2) the model distance and age; this was chosen for simplicity to be representative of the two *NYMG*s. Individual candidates have a range of distances and ages. None the less, the detection limits in both Figs. 8 and 9 correspond to a model derived limiting magnitude of $V \sim 16$ for the lowest mass candidates.

4.3. Undetected Candidates

Three hundred sixty one candidates are undetected by either *ROSAT* or *GALEX*. Fig. 10 shows the V (top) and d_{kin} (bottom) distributions of these candidates. Solid, black and hashed, gray curves represent the undetected candidates (*UC*s) in the *ROSAT* and *GALEX* catalogs respectively. The V distributions show that most *UC*s have $13 \lesssim V \lesssim 15$ and $d_{kin} \gtrsim 50$ pc. These are most likely main sequence stars with kinematics similar to those of the *NYMG*s selected by chance. It is likely that the faintest *UC*s are beyond the detection limits of the surveys. It was expected that $\sim 25\%$ of the candidate sample would be undetected by *GALEX* because of the sky coverage of the *AIS*. However, the greater sensitivity of the *GALEX* satellite is apparent from the distributions. There are fewer undetected candidates overall, the peak of the V distribution is shifted to fainter mags by ~ 1 , and the d_{kin} dis-

⁵Likely new β Pic member PM I04439+3723 is not detected in the *FUV*. S10 estimate the star to be *SpTy* M3 and lie at a distance of ~ 80 pc.

tribution is approximately flat at large distances. The faintest *UCs* in the sample could be pursued for individual follow up to check spectroscopic youth indicators, such as gravity sensitive alkali lines, to verify their suspected main-sequence ages. However, most of the *UCs* appear to be within the estimated limits of the *ROSAT* and *GALEX* surveys and likely represent older stars which only appear to be co-moving with the *BPMG* and *ABDMG* by chance.

Since the *ROSAT* and *GALEX* catalogs do not have uniform coverage of the entire sky we cannot be certain that we have not missed some potentially young stars but the analyses presented are the best way to identify young stars quickly without intensive observation. We recognize that the chosen activity indicators may introduce contamination to the *PYC* sample in the form of flaring dwarfs, unresolved white dwarf-M dwarf systems, and unresolved, tidally interacting binaries and that the reliability of these indicators decreases substantially after $\sim M4$ *SpTy*. To address this problem we devise a simple system to prioritize follow up observations to measure radial velocities and parallaxes.

4.4. Activity, Color, and Priority Indices

Activity Index, A: The 204 *PYCs* have varying levels of activity as indicated by their X-ray, *NUV*, and *FUV* flux ratios. The **A** index shows these variations in a simple way. It is a three digit binary number where each digit represents whether a youth diagnostic is positive (1) or not (0). **A**’s first digit represents the X-ray flux ratio, 1 indicates that the ratio is at or above the *PYC* cut, 0 means that the ratio is either below the cut or X-ray flux is not detected. The second and third digits represent the *NUV* and *FUV* flux ratios respectively. Their value is selected following the same prescription as the first digit. Example activity indices for *PYCs* are listed in Table 2.

Color Index, C: The reliability of the indicators described by **A** is dependent on *PYC* mass. W11 used *SDSS* M-dwarf spectroscopic data to show that the fraction of stars with $H\alpha$ emission increases substantially around mid-M type and nearly all late Ms are active. This is probably the result of convection throughout their interiors and a strengthening of their magnetic dynamos. Since $H\alpha$ traces activity in a way similar to X-ray and UV emission this activity trend can be applied to the indicators described here. Thus, **C** is a single digit binary number indicating whether a star has $(V-K_s) \leq 5$, approximately earlier than M4 according to SDF2000 models, and hence whether **A** is reliable (1) or not (0). We henceforth designate *PYCs* with **C** = 1 as candidates with reliable youth (*CWRYs*) and candidates with **C** = 0 as candidates with ambiguous youth (*CWAYs*). *PYC* color indices are listed in Table 2. The *PYC* sample is comprised of 113 *CWRYs* and 91 *CWAYs*. Even though some *CWAYs* may

actually be active older stars they are still worthy of follow up since the activity cuts have been chosen via comparison to known, young, late-type stars. These candidates are prime targets for studies of gravity sensitive spectral features.

Priority Index, P: The observing priority of a *PYC* can be quickly determined by summing the digits of **A** and **C**. This leads to a new, one digit index **P**, which ranges between 1 - 4 (see Table 2). The most promising candidates, with strong, reliable indication of youth, have **P** = 4. We discuss the statistical properties of the *PYCs* and illustrate the use of their indices when selecting stars for follow up studies in §5.

4.5. Northern *PYC* List

The youth indicator analysis has reduced the number of candidates by nearly 70% to 204 *PYCs*. Inevitably, it still contains contaminants in the form of active stars whose kinematics align with the *NYMGs* by chance. Their removal will require follow up observations that are beyond the scope of this paper. Three stars are candidates for both the *BPMG* and *ABDMG*. Dual candidacy was expected for some stars due to the overlap of the two groups in *U* and *W* velocity space. We present an example of the format of the northern *PYC* list in Table 2 and explain the column designations in the following subsections. The entire list is available in the electronic version of the journal in machine readable format.

Columns 1, 2, and 3 list our internal ID and *Hipparcos* and *Tycho-2* IDs if available. The internal ID is based on the star’s coordinates in the *ICRS* epoch 2000.0 system. The final letter (N, S, E, W) is optional and distinguishes pairs of stars that would otherwise have the same coordinates. The choice depends on the orientation of the pair. If the separation in declination is larger, the stars are appended N and S. If the separation in right ascension is larger, the pair is given E and W. Candidates with NS or EW are not necessarily common proper motion pairs, although they may be. If only one star appears with a directional designation, its counterpart was cut from the sample during the search, usually because it fails to meet the ($V-K_s$) cut.

Columns 4 and 5 list the coordinates in the *ICRS* epoch 2000.0 system. Columns 6 - 9 give the *V*, *J*, *H* and *K_s* photometry of the candidate. If the star is in the *Hipparcos* or *Tycho-2* catalog the *V* mags from those sources are used. If the star is missing from those catalogs the *V* mag is a combination of the USNO-B1.0 (Monet et al. 2003) *B_J*, *R_F*, and *I_F* photographic magnitudes following the conventions of LS05. *J*, *H* and *K_s* magnitudes are from *2MASS*. Columns 10 and 11 list the proper motions of the *PYCs*. Proper motions are taken from the *Hipparcos* and *Tycho-2* catalogs if the candidate has a counterpart, otherwise

the *LSPM*/*SBK* derived proper motions are used. We adopt the ± 8 mas yr $^{-1}$ uncertainty of the *LSPM* and *SBK* catalogs as the proper motion uncertainty in the list.

Columns 12 and 13 list the d_{kin} of the candidate and its uncertainty. Column 14 and 15 list the predicted radial velocity (RV_p , see LS09 and S10) of the candidate and its uncertainty which includes the intrinsic spread in *BPMG* or *ABDMG* *UVW* velocities quoted in §2. Columns 16, 17, and 18 list the logarithm of the X-ray, *NUV*, and *FUV* flux ratios described in §4. Columns 19, 20, and 21 are the activity (A), color (C) and priority (P) indices respectively (see §4) and column 22 identifies whether a star is a *PYC* of the *BPMG* (1) or the *ABDMG* (2). Stars with dual candidacies are listed with identical IDs, coordinates, proper motions, and photometry and differ only in their d_{kin} and RV_p , which are specific to the particular *NYMG*.

5. Statistical Properties

The *PYC* sample is comprised of 49 *BPMG* and 155 *ABDMG* candidates. Figure 11 shows the distributions of the *PYC* *V* mags and d_{kin} with the *BPMG* and *ABDMG* *PYC*s shown in hashed, gray and solid, black histograms respectively. In the *V* mag distributions *BPMG* candidates appear brighter on average. This is most likely due to younger age of the group. The *BPMG* distance distribution also exhibits many fewer candidates at large d_{kin} . Furthermore, the distribution is flat after ~ 50 pc. Brighter candidates at smaller estimated distances make *BPMG* *PYC*s generally more favorable for follow up observations.

5.1. Index Distributions

In this subsection we break the *PYC* sample into subgroups as defined by the A, C, and P indices. We first discuss the color index (C) subgroups and compare their cumulative activity index (ΣA) distributions. Fig. 12 shows the *V* mag (top) and d_{kin} (bottom) distributions for *CWRY*s. The three histograms plotted represent *CWRY*s with $\Sigma A = 1$ (solid, gray), 2 (hashed, dark gray), or 3 (open, red). The largest contribution to the *CWRY* sample are candidates having only one strong activity indicator. These candidates typically have only strong X-ray or *NUV*. It is striking that there are more *CWRY*s with $\Sigma A=3$, those with the strongest indication of youthful activity, than $\Sigma A=2$. The $\Sigma A = 3$ distance distribution also peaks at smaller d_{kin} . The larger number of $\Sigma A=3$ candidates at smaller predicted distances makes follow up of these *CWRY*s particularly pertinent.

The same distributions using the same color designations in Fig. 12 for the *CWAY*s are

shown in Fig. 13. The V distributions are shifted ~ 2 mags fainter than the $CWRYs$. This is expected since $CWAYs$ are systematically redder and represent lower-mass candidates. Like in the $CWRY$ distributions, candidates with $\Sigma A = 1$ dominate, but to a larger degree. However, the number of $CWRYs$ with $\Sigma A = 2$ and $\Sigma A = 3$ is nearly equal. The d_{kin} distribution of $\Sigma A = 3$ $CWAY$ sample is approximately flat. This feature is inconsistent with the other distance distributions in the figure, which have significant peaks at $d_{kin} \geq 60$ pc. The flat distance distribution is indication that contamination does not increase as volume increases in the $\Sigma A = 3$ $CWAY$ sample. Thus these candidates are also prime for follow up.

As a final guide to prioritize follow up, Fig. 14 shows the P index V mag and d_{kin} distributions of the young candidates. The $P = 1$ sample consists entirely of candidates with $(V-K_s) > 5.0$ ($CWAYs$) that have only one strong activity indicator. These candidates are the lowest priority for immediate RV follow up, but are prime targets for the study of gravity sensitive spectral features. The $P = 2$ and 3 distributions are a mixture of $CWRYs$ and $CWAYs$ that may have multiple strong activity indicators. The $P = 4$ distribution consists only of candidates with $(V-K_s) \leq 5.0$ ($CWRYs$) that have strong X-ray, NUV , and FUV flux. These candidates have the strongest indication of reliable youth and are the highest priority for follow up. The $P = 3$ and 4 distance distributions (Fig. 14, bottom) do not have strong peaks beyond 60 pc. This indicates a lower rate of contamination in these samples as volume increases.

5.2. Survey Completeness and Moving Group Densities

Our search for low-mass stars in the $BPMG$ and $ABDMG$ is effectively complete for stars within 70 pc to within the proper motion limit of the SBK catalog. Because the SBK catalog is complete to $V \approx 20$ and has a proper motion limit $\mu > 40$ mas yr $^{-1}$, all low-mass stars within 70 pc will be detected if their absolute V magnitude $M_V < 15.5$ and if their velocity in the plane of the sky $v_{tran} > 13.3$ km s $^{-1}$. Regardless of how much contamination there is in our sample, the fact remains that virtually all moving group members that have absolute magnitudes and velocities within the limits above are to be found in our list.

Not all stars in the $BPMG$ and $ABDMG$ will have proper motions large enough to be detected. To estimate the fraction of stars detected as a function of their distance, we have performed a simple Monte-Carlo simulation which assumes a uniform density of moving group members in the solar vicinity, and estimates how many stars in the synthetic sample would have proper motions large enough to be detected. In addition to the kinematic selection, we add a 5% probability that any star may be overlooked, consistent with the estimated $> 95\%$

completeness of the *SBK* catalog. Results are displayed in Fig. 15 (upper panels) for both the *BPMG* and *ABDMG*; one finds that $>75\%$ of the *BPMG* stars at ≈ 70 pc from the Sun should be on our list, and larger fractions of more nearby objects for a total of $\approx 86.8\%$ of all *BPMG* within 70 pc. For the *ABDMG*, the search is significantly more complete due to the larger systemic velocity of the group, which yields larger proper motions on average than *BPMG* stars. The simulation suggests that $>85\%$ of the *ABDMG* low-mass stars at ≈ 70 pc should be in the list, and $\approx 94.4\%$ of all the members within that range.

With this high level of completeness, it is possible to place firm upper limits on the volume density of *BPMG* and *ABDMG* stars in the northern hemisphere based on the number of stars we identified. We separate the candidates in 10 pc distance bins, count the number of stars with absolute magnitudes $8.0 < M_V < 15.5$ within each bin, and divide this number by the detected fraction as estimated above. We then calculate the density of stars ρ_* in that distance range by dividing by the volume enclosed by each of the corresponding hemispheric shell, and express the result in stars per cubic parsec (stars pc $^{-3}$). Results are displayed in Fig. 15 (lower panels). We calculate ρ_* as a function of distance for the complete list of low-mass star candidates (open triangles) and for the subset of candidates which show strong evidence of youth (*PYC*s, filled squares).

If we believe that all group members should display indicators of youth, while allowing that some non-members might show signs of youth as well, then the mean density of young candidates sets an upper limit for the density of the group. Under this assumption, we find that in the northern sky volume within 70 pc of the Sun, the *BPMG* has a maximum number density of low-mass stars of $\approx 6.7 \times 10^{-5}$ stars pc $^{-3}$, which means that the same volume should be host to at most ≈ 36 low-mass (M dwarf) members of the *BPMG*. For the *ABDMG*, we find that the group has a maximum density of $\approx 2.2 \times 10^{-4}$ stars pc $^{-3}$ for low-mass stars, which suggests that the 70 pc volume should contain at most ≈ 119 low-mass (M dwarf) members. We expect that most of the true low-mass, north-sky members of the *BPMG* and *ABDMG* should be in our Table 2.

6. Preliminary Results

6.1. Ultracool Candidates

Seven candidates in Fig. 7 are redder in ($H-K_s$) than the expected dwarf sequence (black box). These stars are potential ultracool candidates with *SpTy*'s M7 and later. We perform a literature search for pertinent youth and kinematic data regarding these candidates since they are not expected to exhibit strong activity. The literature reveals three *LNMs*, another

three stars that require further follow up, and one that is ruled out on the basis of inconsistent *RVs* (see Table 3).

6.2. *PYC*s with *Hipparcos* Distances

Five stars in the *PYC* sample have distances measured by *Hipparcos*, this allows us to directly test group membership by verifying that d_{kin} is consistent with the parallax distance (d_π). We have calculated distances for all stars listed in the *Hipparcos* catalog based on measured parallaxes from the recent new reduction by van Leeuwen (2007). Table 4 compiles literature data on these 5 stars and lists their ID, *Hipparcos* ID, coordinates in the *ICRS* system, *V* mags, *2MASS* K_s mags, predicted d_{kin} and measured d_π distances, predicted and measured *RV*, *NYMG* candidacy, and if the star was removed from the sample. 5 *LNMs* (1 triple system and 2 singles) are identified, and 2 are ruled out on the basis of inconsistent measured *RV* (see Table 4). All of the candidates with *Hipparcos* distances are *CWRYs* with $P = 3$ or 4.

6.3. Likely New Members

PYC J09362+3731 = HIP 47133: HIP 47133 is a late-K dwarf at a distance of 31 pc, consistent with our predicted distance. The star exhibits strong *NUV*, and *FUV* emission, consistent with known late type *BPMG* members. We identify HIP 47133 as a likely new member of the *BPMG* on the basis of consistent distance and strong activity. *RV* measurements should be performed to confirm membership.

PYC J10143+2104 = HIP 50156: HIP 50156 is an M1 dwarf at a distance of ~ 20 pc. Strong X-ray flux, moderate $H\alpha$ emission, possible low surface gravity from CaH indices, but no 6708 Å lithium line are described by Sh09. We identify strong *NUV* and *FUV* flux as well. López-Santiago et al. (2010, hereafter L10) measure an *RV* of 2.7 ± 1.0 km s $^{-1}$, which matches well with our predicted *RV*, and calculate $(UVW) = (-6.8, -18.3, -8.2)$. L10 classify the star as a member of the local association and also report a Li non-detection. However, the (UVW) velocities are more consistent with those of the *BPMG* than those of the local association (Montes et al. 2001). The lack of detected Li in both Sh09 and L10 is contrary to expectations for ~ 10 Myr old early-M dwarfs. But, BC10 suggest that Li content is not a reliable youth indicator since it is strongly affected by stellar accretion history. We therefore identify HIP 50156 as a likely member of the *BPMG* based on consistent *UVW* kinematics and strong activity and suggest further follow up for confirmation.

PYC J01036+4051 = HIP 4967: HIP 4967 is a visual triple system at a distance of ~ 30 pc. Sh09 identify indicators of youth in the spectra of the M3 secondary and M4 tertiary components, including H α emission, and estimate the ages to be 20 - 300 Myr. We also identify strong activity in components of the system. Based on evidence of youth and consistent distance we identify HIP 4967 as a likely member of the *ABDMG*. *RV* measurements should be pursued to verify membership.

PM I00194+4614 = 2MASS J0019262+461407: *2MASS* J0019262+461407 (hereafter 2M0019) was identified by Cruz et al. (2003) as an M8 dwarf in a search for nearby ultracool objects in the *2MASS* catalog. Reiners & Basri (2009, 2010, hereafter RB09,10) measure an *RV* of -19.5 ± 2.0 km s $^{-1}$, which is consistent with our predicted *RV*, and a remarkably large *vsini* of 68 ± 10 km s $^{-1}$. In their high resolution optical spectra they also identify lithium at 6708 Å in absorption, indicating that 2M0019 is most likely a young brown dwarf ($M \lesssim 65 M_{Jup}$, Age < 0.5 Gyr). We identify 2M0019 as a *LNM* of the *ABDMG* based on indicators of youth and consistent *RV*. Assignment as a true group member awaits parallax measurement to verify that d_{kin} is the true distance and a more detailed analysis of youth indicators.

PM I04436+0002 = 2MASS J0443376+000205: *2MASS* J0443376+000205 (hereafter 2M0443) was identified as an M9 dwarf by Hawley et al. (2002). Cruz et al. (2007) identified indicators of low surface gravity in its spectrum and propose that the object is a young brown dwarf. The *RV* and *vsini* of 2M0443 were measured by RB09 and RB10 to be 17.1 ± 2.0 km s $^{-1}$ and 13.5 ± 2.0 km s $^{-1}$ respectively. The *RV* measurement is consistent with our predicted *RV*. Reiners and Basri also identify lithium absorption in the dwarf, strengthening the argument that 2M0443 is a young brown dwarf. Thus, we identify 2M0443 as a *LNM* of the *ABDMG* and will pursue a parallax measurement to verify membership.

PM I13143+1320 = 2MASS J1314203+132001: *2MASS* J1314203+132001 (hereafter 2M1314) was first identified as the high proper motion star NLTT 33370 by Luyten (1979). Based on its photometry, LS05 estimate its distance to be 9.7 ± 3.0 pc. Lépine et al. (2009, hereafter L09) measure strong H α emission (EW = 54.1 Å) and a parallactic distance of 16.4 ± 0.8 pc. This is nearly twice the photometric distance but in agreement with our predicted d_{kin} . Since d_{phot} significantly underestimates the true distance to 2M1314 the star could be an unresolved binary or very young. Either of these scenarios can be consistent with the strong H α emission. If 2M1314 is $\lesssim 100$ Myr old its mass would be very close to the substellar limit. We identify 2M1314 as a *LNM* of the *ABDMG* based on the evidence in the literature and will pursue *RV* measurements and follow up on further indicators of youth in order to verify group membership.

If these three ultracool *LNMs* are verified to be bona fide members of the AB Dor group they will be the lowest mass, isolated members and represent important benchmarks.

7. Summary

We have presented a list of 204 young moving group candidates in the northern hemisphere. These stars are candidates of the ~ 10 Myr old β Pictoris moving group and ~ 70 Myr old AB Doradus moving group. Candidates were selected from the *Tycho-2*, *LSPM-North*, and *SBK* catalogs using the search algorithm first described in LS09 and S10. Selection criteria used in choosing candidates were derived from the known members of the *NYMGs*. X-ray, *NUV*, and *FUV* activity indicators were used to trim the initial sample to only the young stars following the convention of Sh09 and Sh11. Identification of true moving group members in the list requires *RV* and parallax measurements to verify consistent group kinematics. We have devised a simple system of indices based on activity and color to help prioritize follow up observations.

From detailed inspection and data gathered in the literature, we can identify 2 *LNMs* of the *BPMG* and six of the *ABDMG* (3 in a triple system). Three of the *LNMs* of the *ABDMG* are possible young brown dwarfs. The identification of 3 *LNMs* as possible brown dwarfs is particularly valuable because if follow up proves them true members of the group they will be the lowest-mass, isolated members of the group yet identified. Not only are these objects interesting for assessing the substellar mass function of the *ABDMG*, they may represent benchmark young substellar objects which are crucial for understanding substellar formation and evolution. Our proper motion search technique has now yielded at least 24 likely new moving group members (LS09, S10, this work).

This paper concerns only candidates of the *BPMG* and *ABDMG* north of the celestial equator. Since 80 to 90% of the known β Pic and AB Dor group members lie in the south (see T08), we can expect that extension of our identification procedures to the south will yield similarly greater numbers of *PYCs* and *LNMs*. A complete census of *NYMG* members including the low-mass stars will allow for the study of: 1) the origins of the moving groups, 2) stellar evolution in a relatively nearby sample of *PTTSs* and young brown dwarfs and, 3) exoplanets and their formation.

We thank the referee for helpful comments that improved this manuscript. We thank C. Bender for sharing with us his software for the extraction of CSHELL spectra and for their analysis by correlation techniques. The work of J.E.S and M.S. was supported in part by NSF grant AST 09-07745. The work of S.L. was supported by NSF grants AST 06-07757 and AST 09-08406. This publication makes use of data products from the Two Micron All Sky Survey, which is a joint project of the University of Massachusetts and the Infrared

Processing and Analysis Center/California Institute of Technology, funded by the National Aeronautics and Space Administration and the National Science Foundation. This research has made use of the SIMBAD database, Aladin, and VizieR, operated at CDS, Strasbourg, France.

REFERENCES

- Baraffe, I. and Chabrier, G., 2010, A&A, 521, 44.
- Bessell, M. S. and Brett, J. M., 1988, PASP, 100, 1134.
- Bessell, M. S., 1991, AJ, 101, 662.
- Bochanski, J. J., Hawley, S. L., Covey, K. R., West, A. A., Reid, I. N., Golimowski, D. A., and Ivezić, Ž., 2010, AJ, 139, 2679.
- Cruz, K. L., Reid, I. N., Liebert, J., Kirkpatrick, J. D., and Lowrance, P. J., 2003, AJ, 126, 2421.
- Cruz, K. L. et al., 2007, AJ, 133, 439.
- Fernández, D., Figueras, F., and Torra, J., 2008, A&A, 480, 735.
- Findeisen, K. and Hillenbrand, L., 2010, AJ, 139, 1338.
- Gizis, J. E., Monet, D. G., Reid, I. N., Kirkpatrick, J. D., Liebert, J., Williams, R. J., 2000, AJ, 120, 1085.
- Greene, T. P., Tokunaga, A. T., Toomey, D. W., and Carr, J. B., 1993, Proc. SPIE, 1946, 313.
- Hawley, S. et al., 2002, AJ, 123, 3409.
- Herbig, G., 1978, in *Problems of Physics and Evolution of the Universe.*, Ed. L.V. Mirzoyan. Yerevan Publishing.
- Høg, E., Fabricius, C., Makarov, V.V., Urban, S., Corbin, T., Wycoff, G., Bastian, U., Schwekendiek, P., and Wicenec, A., 2000, A&A, 355, L27.
- Johnson, D. R. H and Soderblom, D. R., 1987, AJ, 93, 864.
- Kiss, L. L., et al., 2011, MNRAS, 411, 117.
- Lasker, B. M., et al., 2008, AJ, 136, 735.
- Lépine, S. and Shara, M., 2005, AJ, 189, 1483.
- Lépine, S. and Simon, M. 2009, AJ, 137, 3632.
- Lépine, S., Thorstensen, J. R., Shara, M. M., and Rich, R. M., 2009, AJ, 137, 4109.

- López-Santiago, J. et al., 2010, A&A, 514, 97.
- Luyten, W. J., 1979, *New Luyten Two Tenths Catalogue*, University of Minnesota, Minneapolis, Vol. 2.
- Mamajek, E. E. and Feigelson, E. D., 2001, ASP Conference Series, Ed. R. Jayawardhana and T. Greene, Volume 244, 104.
- Martin, D. C., et al., 2005, ApJ, 619, L1.
- Monet, D. G., et al., 2003, AJ, 125, 984.
- Montes, D., López-Santiago, J., Fernández-Figueroa, M. J., and Gálvez, M. C., 2001, A&A, 379, 976.
- Morrissey, P., et al., 2005, ApJL, 619, 7.
- Palla, F. and Randich, S., 2004, arXiv:astro-ph/0412212v1.
- Perryman, M. A. C., et al., 1997, A&A, 323, L49.
- Reid, I. N., Kirkpatrick, J. D., Liebert, J., Gizis, J. E., Dahn, C. C., and Monet, D. G., 2002 AJ, 124, 519.
- Reiners, A., and Basri, G., 2009, ApJ, 705, 1416.
- Reiners, A., and Basri, G., 2010, ApJ, 710, 924.
- Rice, E. L., Faherty, J. K., and Cruz, K. L., 2010, ApJL, 715, L165.
- Rice, E. L., et al., 2011, arXiv1101.4231v1.
- Rodriguez, D. R., Bessell, M. S., Zuckerman, B., and Kastner, J. H., 2011, ApJ, 727, 62.
- Schlieder, J. E., Lépine, S., and Simon, M., 2010, AJ, 140, 119.
- Schlieder, J. E., Lépine, S., Rice, E., Simon, M., Fielding, D., and Tomasino, R., 2011, AJ, submitted
- Schmitt, J. H. M. M., Fleming, T. A., and Giampapa, M. S., 1995, ApJ, 450, 401.
- Shkolnik, E., Liu, M. C., and Reid, I. N., 2009, ApJ, 699, 649.
- Shkolnik, E., Liu, M. C., Reid, I. N., Dupuy, T., and Weinberger, A. J., 2011, ApJ, 727, 6.
- Siess, L., Dufour, E. & Forestini, M. 2000, A&A, 358, 593

- Skrutskie, M. F., et al., 2006, AJ, 131, 1163.
- Steinmetz, M., et al., 2006, AJ, 132, 1645.
- Torres, C. A. O., Quast, G. R., Melo, C. H. F., and Sterzik, M. F., 2008, in *Handbook of Star Forming Regions*, Vol. II, Ed. B. Reipurth.
- Uppgren, A. R. and Harlow, J. J. B., 1996, PASP, 108, 64.
- van Leeuwen, F., 2007, A&A, 474, 653 .
- Voges, W., et al., 1999, A&A, 349, 389.
- Voges, W., et al., 2000, IAUC, 7432, 1.
- West, A. A., Hawley, S. L., Bochanski, J. J., Covey, K. R., Reid, I. N., Dhital, S., Hilton, E. J., and Masuda, M., 2008, AJ, 135, 785.
- West, A. A., et al., 2011, AJ, 141, 97.
- Zuckerman, B. & Song, I., 2004, ARA&A, 42, 685.

Table 1
Recovered Known NYMG Members

Cat ID	<i>Hip.</i> ID	<i>Tycho2</i> ID	$\alpha(ICRS)$ (2000.0)	$\delta(ICRS)$ (2000.0)	V (mag)	K_s (mag)	d_{kin} (pc)	$SpTy^a$	Membership
PM I02414+0559	12545		40.357864	5.988454	10.3	7.1	38.5±3.7	K6Ve	<i>BPMG</i>
PM I04595+0147	23200	85 1075 1	74.895126	1.783535	10.3	6.3	25.8±2.9	M0Ve	<i>BPMG</i>
PM I17386+6114	86346	4199 1286 1	264.665100	61.237804	10.3	6.8	24.2±5.1	K7Ve	<i>ABDMG</i>
PM I21521+0537	107948	556 1289 1	328.043396	5.626641	12.1	7.4	29.9±2.0	M2Ve	<i>ABDMG</i>
PM I22234+3227	110526	2738 1390 1	335.871185	32.459461	10.7	6.1	15.0±1.1	M3e	<i>ABDMG</i>
PM I23060+6355	114066	4286 212 1	346.520111	63.926220	10.9	7.0	23.7±2.0	M1e	<i>ABDMG</i>

^a*SpTy*'s from T08

Table 2
Northern PYC List

PYC ID	<i>Hip.</i> ID	<i>Tycho2</i> ID	$\alpha(ICRS)$ (2000.0)	$\delta(ICRS)$ (2000.0)	<i>V</i> (mag)	<i>J</i> (mag)	<i>H</i> (mag)	<i>K_s</i> (mag)	μ_α (mas yr ⁻¹)	μ_δ (mas yr ⁻¹)	<i>d_{kin}</i> (pc)	δd_{kin} (pc)	<i>RV_p</i> (km s ⁻¹)	δRV_p (km s ⁻¹)	[<i>X</i>] ^a (dex)	[<i>N</i>] ^b (dex)	[<i>F</i>] ^c (dex)	A	C	P	Cand. ^d
J00025+3422N			0.645568	34.381161	13.6	10.4	9.7	9.5	67.0	-52.0	68.8	7.4	-14.11	1.31	0.00	-3.80	-4.23	011	1	3	2
J00197+1951			4.929336	19.853241	15.7	10.7	10.1	9.9	59.0	-45.0	59.4	7.9	-1.73	1.05	-1.74	-3.86	0.00	110	0	2	1
J00270+6630			6.761791	66.510834	13.2	9.6	8.9	8.7	66.0	-23.0	56.9	8.3	-9.16	1.27	-2.36	0.00	0.00	100	1	2	1
J00270+6630			6.761791	66.510834	13.2	9.6	8.9	8.7	66.0	-23.0	69.5	9.0	-20.81	1.23	-2.36	0.00	0.00	100	1	2	2
J00325+0729			8.145008	7.490874	12.8	8.4	7.8	7.5	92.0	-55.0	41.1	4.4	1.70	1.05	-1.60	-3.86	-4.47	111	0	3	1
J00390+1330			9.764313	13.504687	15.7	10.9	10.4	10.1	66.0	-70.0	67.7	6.4	-3.45	1.45	-1.97	-3.79	-3.96	111	0	3	2
J00411+5523			10.296559	55.399475	16.6	11.4	10.8	10.6	84.0	-61.0	51.7	4.9	-17.76	1.24	-1.60	0.00	0.00	100	0	1	2
J00450+2634			11.250682	26.569508	12.5	9.5	8.9	8.7	85.0	-100.0	48.2	3.7	-8.06	1.37	-2.02	-3.65	0.00	110	1	3	2
J00484+3632		2288 758 1	12.119358	36.542927	11.7	9.2	8.6	8.5	59.0	-40.0	61.4	8.4	-3.14	1.25	0.00	-3.90	0.00	010	1	2	1
J00489+4435			12.242649	44.585823	13.9	9.1	8.5	8.2	116.0	-136.0	32.6	2.2	-14.15	1.27	-1.65	0.00	0.00	100	0	1	2
J00495+0356			12.394575	3.938275	14.8	10.9	10.3	10.0	71.0	-88.0	57.9	4.8	1.35	1.51	0.00	-3.90	0.00	010	1	2	2
J00546+3434			13.671499	34.575741	15.4	10.9	10.3	10.1	60.0	-68.0	68.1	6.8	-10.30	1.32	0.00	-3.89	0.00	010	0	1	2
J01028+1856			15.712469	18.948402	14.4	9.5	8.9	8.7	94.0	-53.0	40.9	4.4	1.53	1.23	0.00	-3.90	-4.36	011	0	2	1
J01036+4051	4967	2803 800 1	15.917160	40.858143	10.9	8.1	7.5	7.3	122.0	-167.0	29.2	1.8	-11.93	1.29	-2.05	-3.51	-4.38	111	1	4	2
J01037+4051W			15.925412	40.854427	13.5	9.4	8.8	8.5	132.0	-164.0	28.7	1.8	-11.93	1.29	-1.57	-3.83	-4.44	111	1	4	2

Note: This table is available in its entirety in machine readable format in the online version of the journal. This portion is given as an example of format and content.

^alog(F_X/F_{Ks}).

^blog(F_{NUV}/F_{Ks}).

^clog(F_{FUV}/F_{Ks}).

^dCandidate of (1) *BPMG*, (2) *ABDMG*.

Table 3
Ultracool Candidates

Cat ID	2MASS ID	$\alpha(ICRS)$ (2000.0)	$\delta(ICRS)$ (2000.0)	V (mag)	J (mag)	H (mag)	K_s (mag)	d_{kin} (pc)	d_π (pc)	d_{phot} (pc)	RV_p (km s ⁻¹)	RV_m (km s ⁻¹)	$SpTy$	Cand.	Notes
Likely New Members															
PM I00194+4614	J0019262+461407	4.859472	46.235477	20.0	12.6	11.9	11.5	39.6±3.1		19.5±1.6 ^a	-16.5±1.3	-19.5±2.0 ^b	M8 ^a	ABDMG	$RV_p \approx RV_m$, youth ^{b,c}
PM I04436+0002	J0443376+000205	70.906723	0.034731	19.6	12.5	11.8	11.2	39.5±3.1		16.2±1.0 ^d	19.0±1.4	17.1±2.0 ^b	M9 ^d	ABDMG	$RV_p \approx RV_m$, youth ^{b,d}
PM I13143+1320	J1314203+132001	198.584839	13.333536	15.9	9.8	9.2	8.8	20.1±1.0	16.4±0.8 ^g	9.7±3.0 ^g	-10.3±1.6		M7 ^g	ABDMG	$d_{kin} \approx d_\pi$, youth ^g
Require Further Followup															
PM I03010+4416	J0301032+441656	45.263393	44.282410	18.0	12.1	11.4	11.0	50.6±3.9		24.5±4.2 ^a	-6.4±1.3		M6 ^a	ABDMG	25
PM I09069+0301	J0906955+030117	136.733276	3.021399	14.6	11.1	10.5	10.1	65.6±6.8			14.0±1.4			ABDMG	
PM I15291+6312	J1529101+631253	232.292389	63.214989	19.5	11.6	10.9	10.6	21.7±2.4			-27.6±1.4			ABDMG	
Ruled Out															
PM I08109+1420	J0810586+142039	122.744370	14.344112	19.6	12.7	12.1	11.6	46.0±3.6		13.8±2.1 ^e	11.9±1.3	27.4±0.4 ^e	M9 ^f	ABDMG	$RV_p \not\approx RV_m$

^aCruz et al. (2003)
^bA. Reiners & G. Basri (2009)
^cA. Reiners & G. Basri (2010)
^dCruz et al. (2007)
^eReid et al. (2002)
^fGizis et al. (2000)
^gLépine et al. (2009)

Table 4
Candidates With Consistent Hipparcos Distances

PYC ID	<i>Hip.</i> ID	$\alpha(ICRS)$ (2000.0)	$\delta(ICRS)$ (2000.0)	V (mag)	K_s (mag)	d_{kin} (pc)	d_π^a (pc)	RV_p (km s ⁻¹)	RV_m (km s ⁻¹)	<i>SpTy</i>	Cand.	Notes
Likely New Members												
J01036+4051	4967	15.917160	40.858143	10.9	7.3	29.2±1.8	29.9±2.1	-11.9±1.3		~M ^b	<i>ABDMG</i>	VT ^b
J09362+3731	47133	144.066330	37.529320	11.1	7.2	33.0±2.9	33.7±2.6	1.0±1.6		K5 ^c	<i>BPMG</i>	
J10143+2104	50156	153.579926	21.074898	10.0	6.3	20.7±1.7	23.1±1.0	2.8±1.3	2.7±0.1 ^d	M1 ^b	<i>BPMG</i>	RV _{<i>p</i>} ≈ RV _{<i>m</i>}
Ruled Out												
J12198+5246	60121	184.950302	52.779182	11.1	7.5	25.0±1.6	28.0±1.7	-18.6±1.5	-4.9±1.2 ^e	K7 ^c	<i>ABDMG</i>	RV _{<i>p</i>} $\not\approx$ RV _{<i>m</i>}
J12576+3513S	63253	194.417801	35.225014	10.6	6.6	17.6±0.9	19.3±1.1	-16.3±1.6	-9.5±0.6 ^f	M4 ^b	<i>ABDMG</i>	RV _{<i>p</i>} $\not\approx$ RV _{<i>m</i>} , VB ^b

^adistance from *Hipparcos* new reduction parallax (van Leeuwen 2007)

^bVT = visual triple, VB = visual binary; Shkolnik et al. (2009)

^cSpTy from SIMBAD

^dLópez-Santiago et al. (2010)

^eUpgren et al. (1996)

^fThis work, using CSHELL at the NASA-IRTF (Greene et al. 1993)

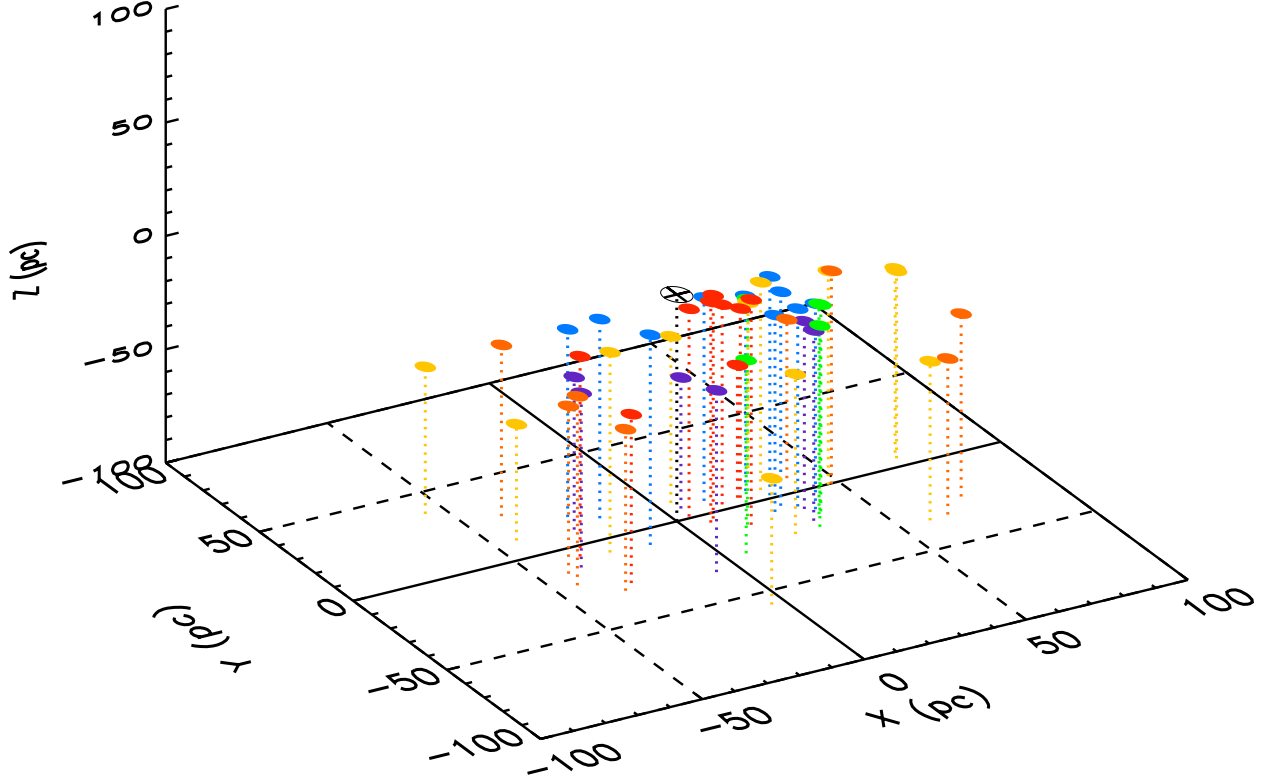


Fig. 1.— *BPMG* *XYZ* distribution, colors represent increments of $(V-K_s)$ color, a rough indicator of mass. From Siess et al. (2000) models, colors are approximately: violet = $1.7 \leq (M/M_\odot) < 2.0$ (A *SpTy*'s); blue = $1.4 \leq (M/M_\odot) < 1.7$ (F *SpTy*'s); green = $0.9 \leq (M/M_\odot) < 1.4$ (G - mid-K *SpTy*'s); yellow = $0.6 \leq (M/M_\odot) < 0.9$ (late-K - early-M *SpTy*'s); orange = $0.3 \leq (M/M_\odot) < 0.6$ (mid-M *SpTy*'s); red = $(M/M_\odot) < 0.3$ ($>M5$ *SpTy*). The large cross at $(X,Y,Z) = (0, 0, 0)$ represents the Sun. The *BPMG* shows extension in the *X* direction, the direction toward the galactic center, a common feature among younger *NYMGs* (T08).

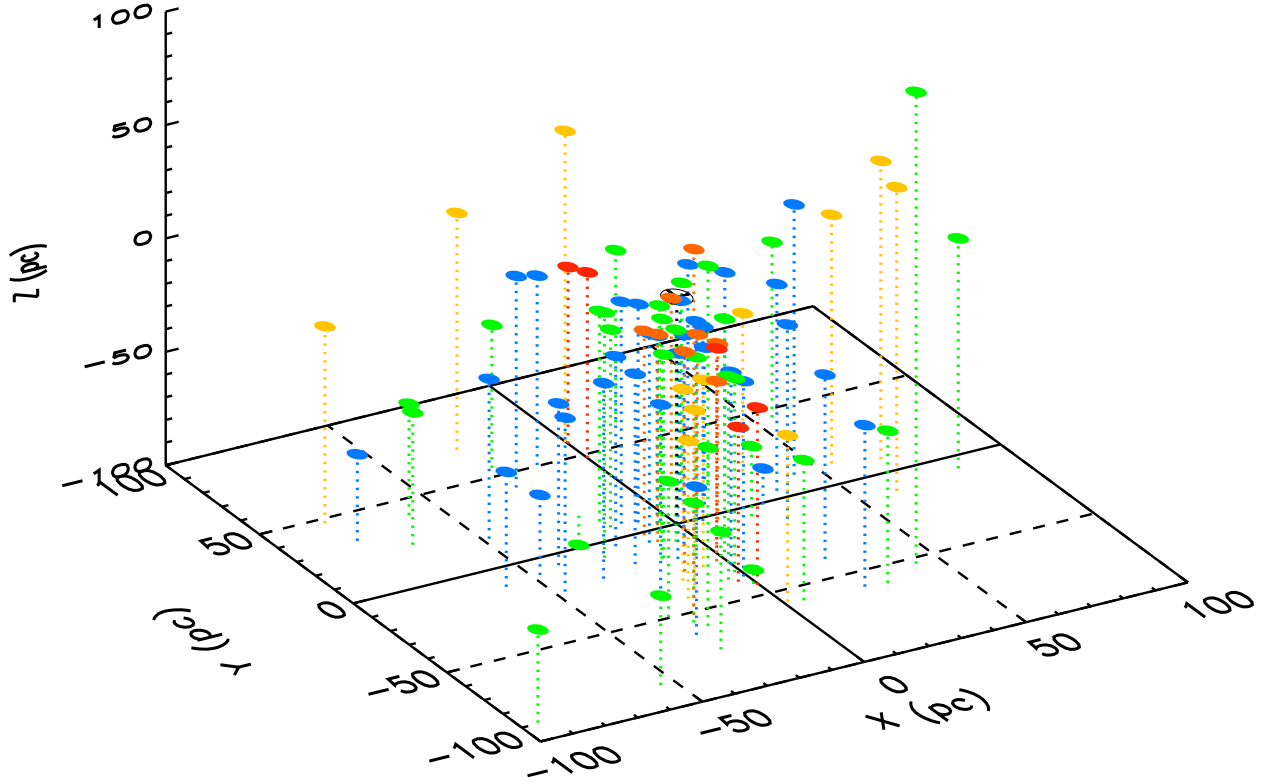


Fig. 2.— *ABDMG* *XYZ* distribution, symbols are identical to Fig. 1. The *ABDMG* has a roughly uniform distribution and lacks the *X* direction extension of the younger *BPMG*, this feature may be due to its older age. The lowest mass stars are near the Sun, probably a selection effect due to their low luminosities.

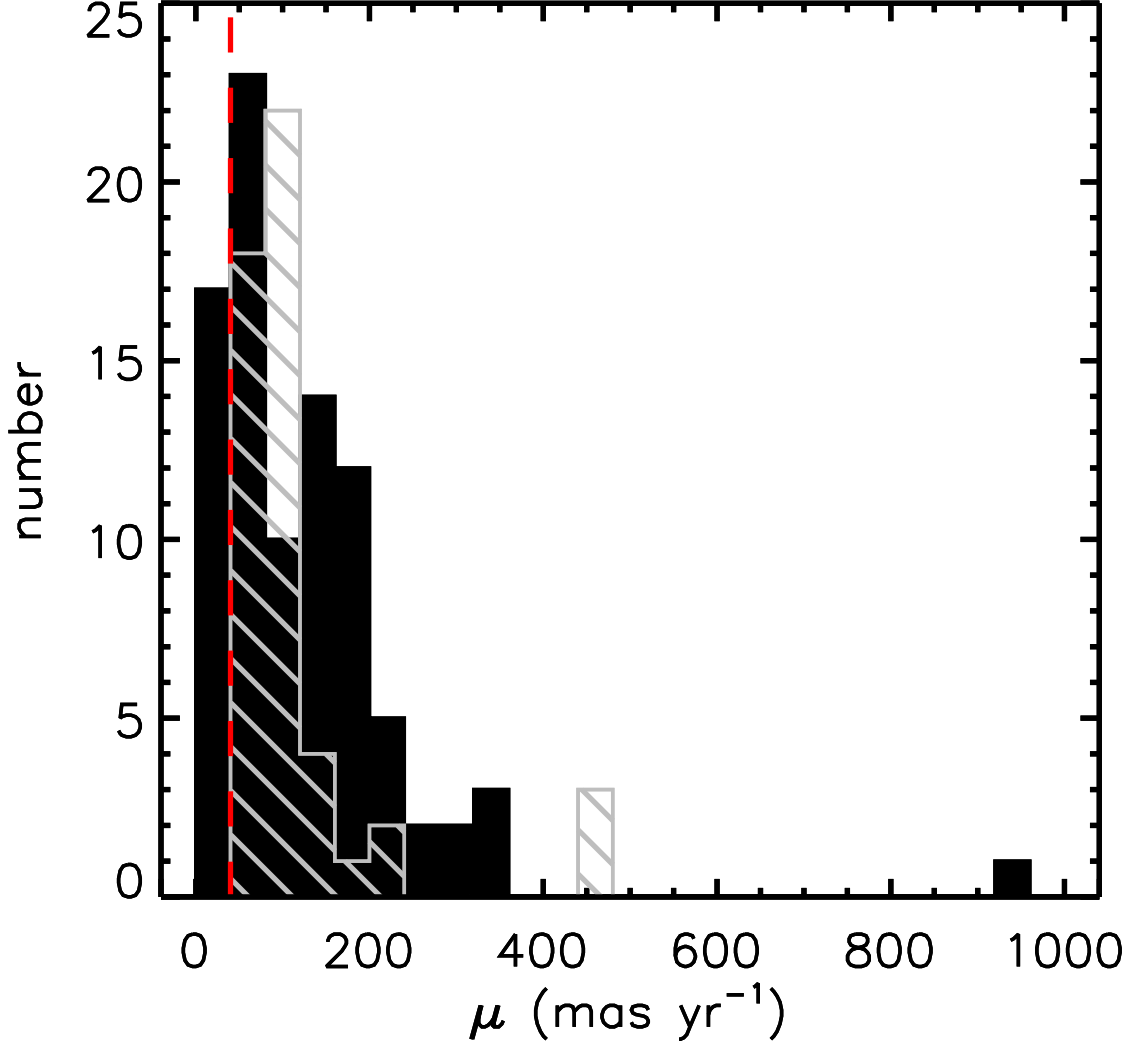


Fig. 3.— Proper motion distributions of the known members of the *BPMG* (gray, hashed) and *ABDMG* (black, solid). The larger spread in proper motions of *ABDMG* members is in part due to the larger space motion of the group, but may also be due to a larger spatial extension of the group due to its older age. The dashed red line at $\mu = 40 \text{ mas yr}^{-1}$ represents the lower proper motion limit in our candidate search. Most known members in the northern hemisphere have $\mu \geq 40 \text{ mas yr}^{-1}$. A color version of this figure is available in the electronic journal.

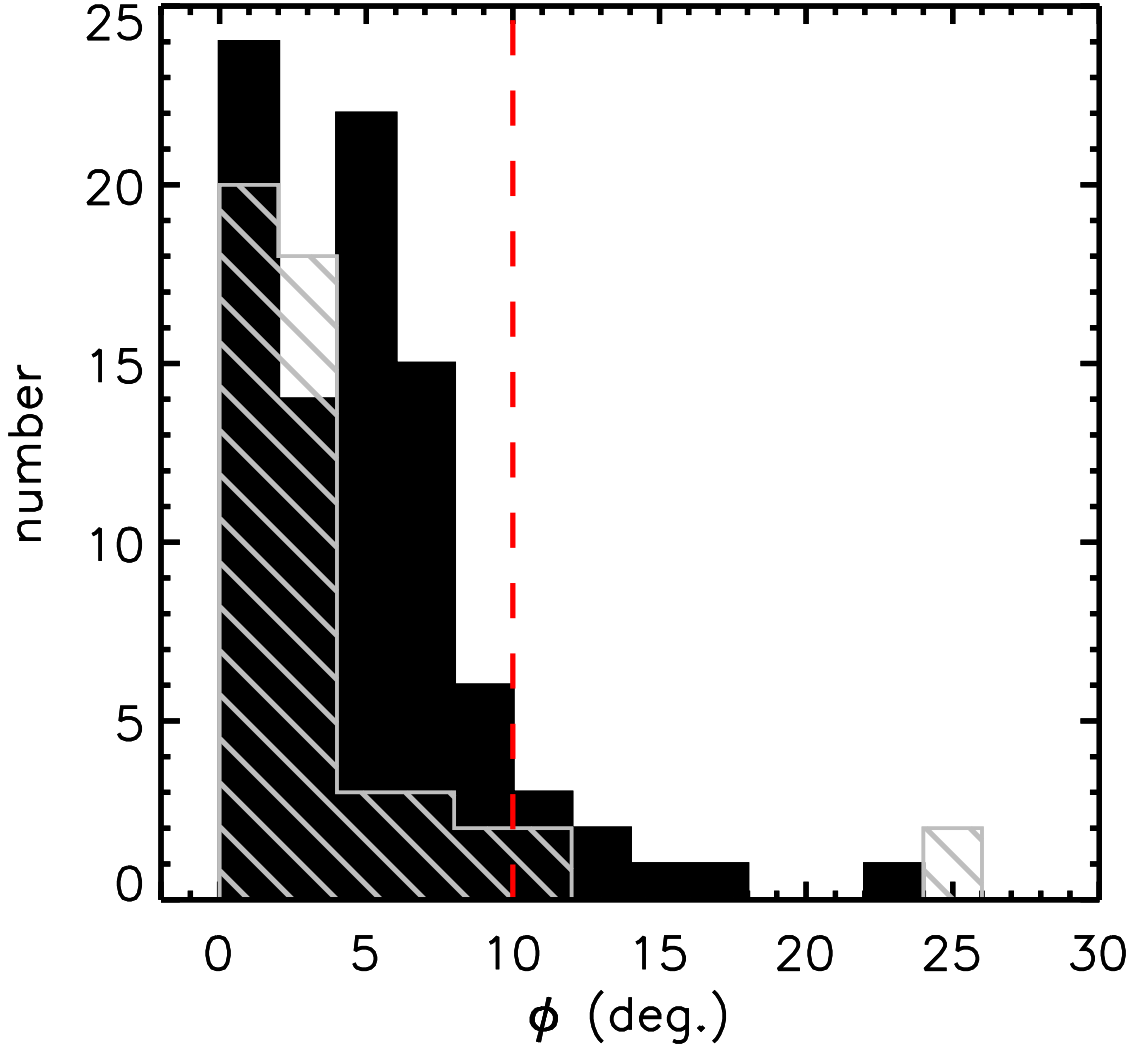


Fig. 4.— ϕ distributions of the known members of the *BPMG* and *ABDMG*. Color designations are the same as Fig. 3. The red dashed line at $\phi = 10^\circ$ is the upper ϕ limit of our search. A color version of this figure is available in the electronic journal.

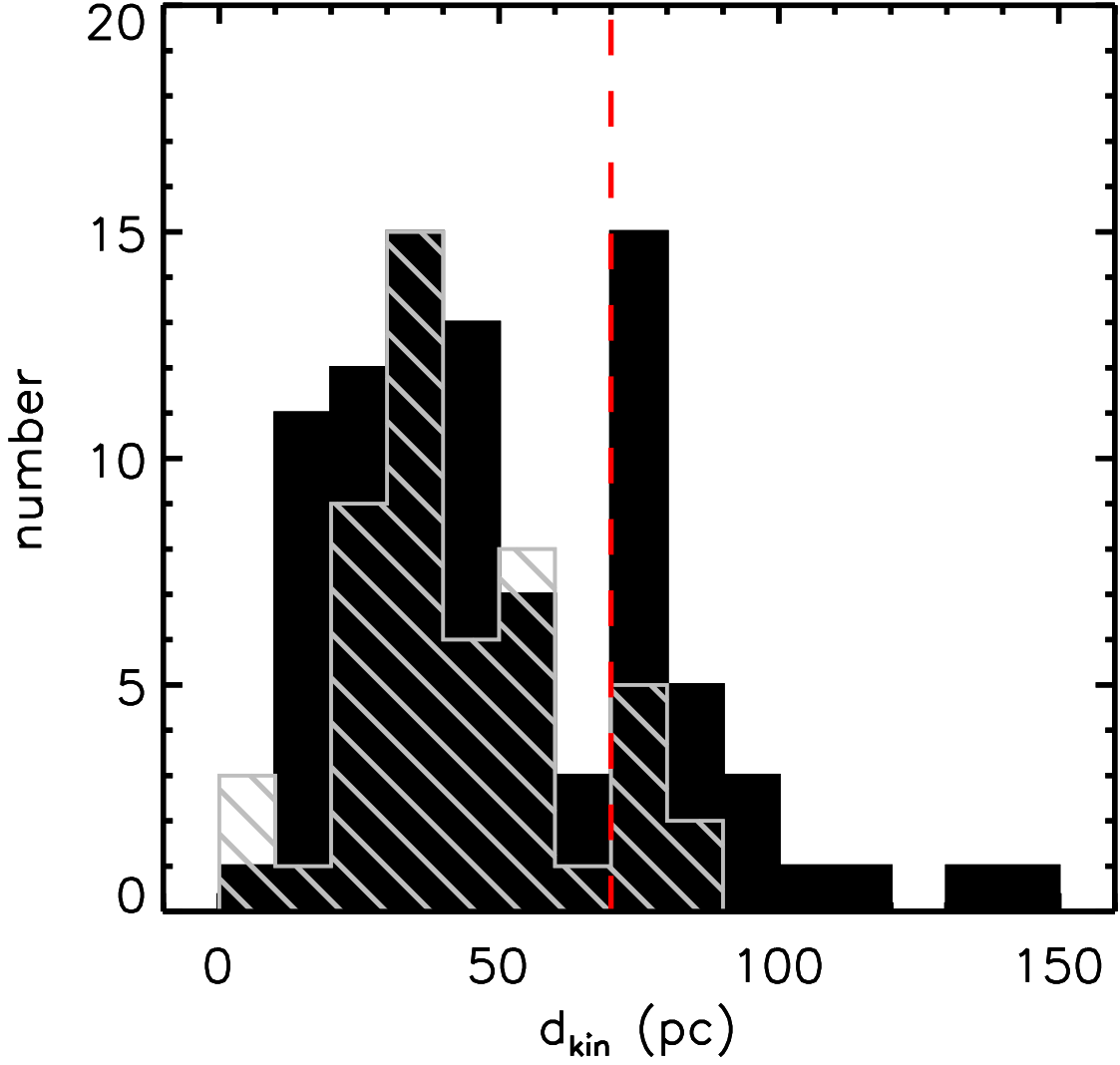


Fig. 5.— d_{kin} distributions of the known members of the *BPMG* and *ABDMG*. Color designations are the same as Fig. 3. Since known *NYMG* members are plotted, d_{kin} is the true distance. We choose 70 pc as the upper d_{kin} limit of our candidate search (dashed red line). A color version of this figure is available in the electronic journal.

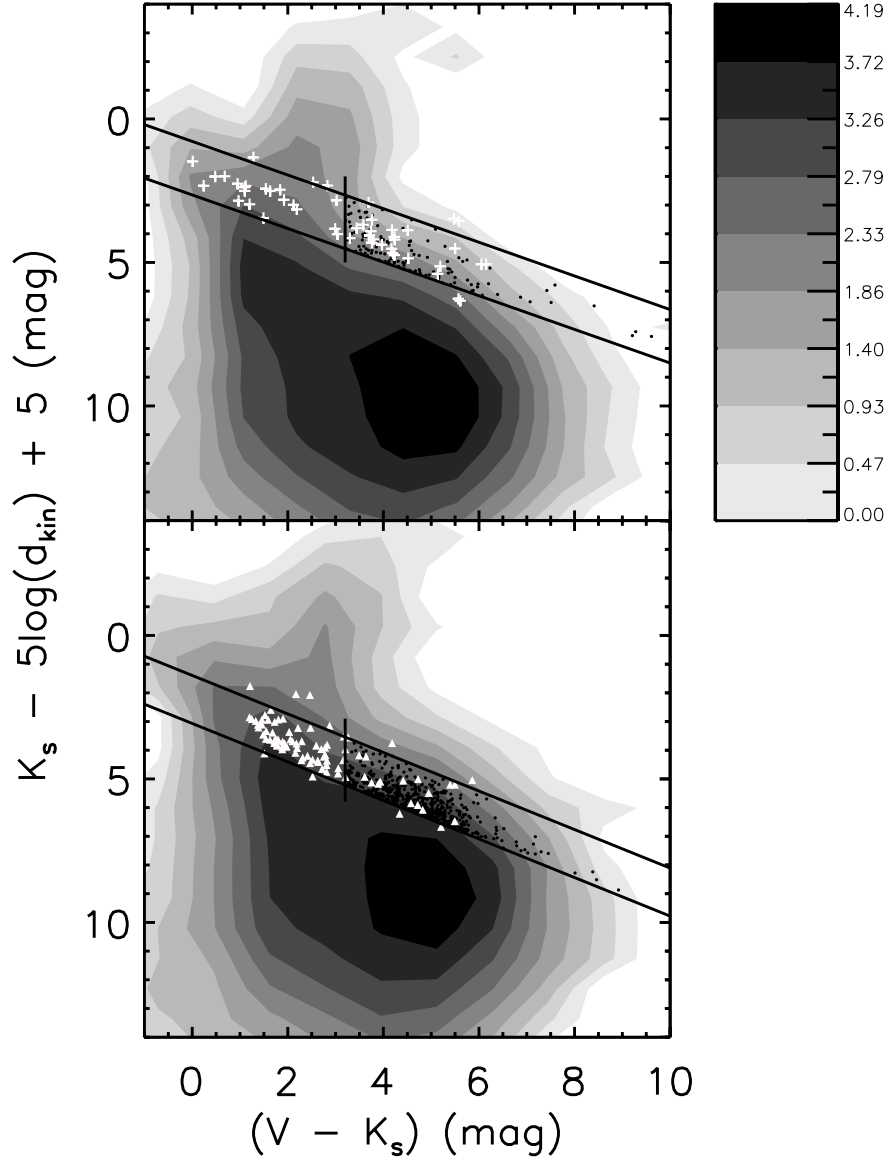


Fig. 6.— Color-magnitude diagrams for *BPMG* (top) and *ABDMG* (bottom) candidates in the *Tycho-2*, *LSPM*, and *SBK* catalogs. M_K was calculated using candidate d_{kin} . Shaded contours represent stars whose proper motions are consistent with group membership. The shading is defined by the logarithm of the number density of these stars in M_K vs. $(V - K_s)$ space. The logarithmic scale is given by the vertical bar to the right of the top plot. White crosses and solid triangles represent known members of the respective groups. The parallel black lines indicate a 2σ uncertainty in a least-squares linear fit to the *NYMG* cluster sequence, any star falling outside of the lines is rejected from the sample. The vertical bar at $(V - K_s) = 3.2$ indicates the color cut imposed in order to select stars later than $\sim K5$ and avoid the inclusion of giants. Candidates selected by the search algorithm are represented by black dots, these are stars surviving all cuts imposed in the search, including $d_{kin} \leq 70$ pc.

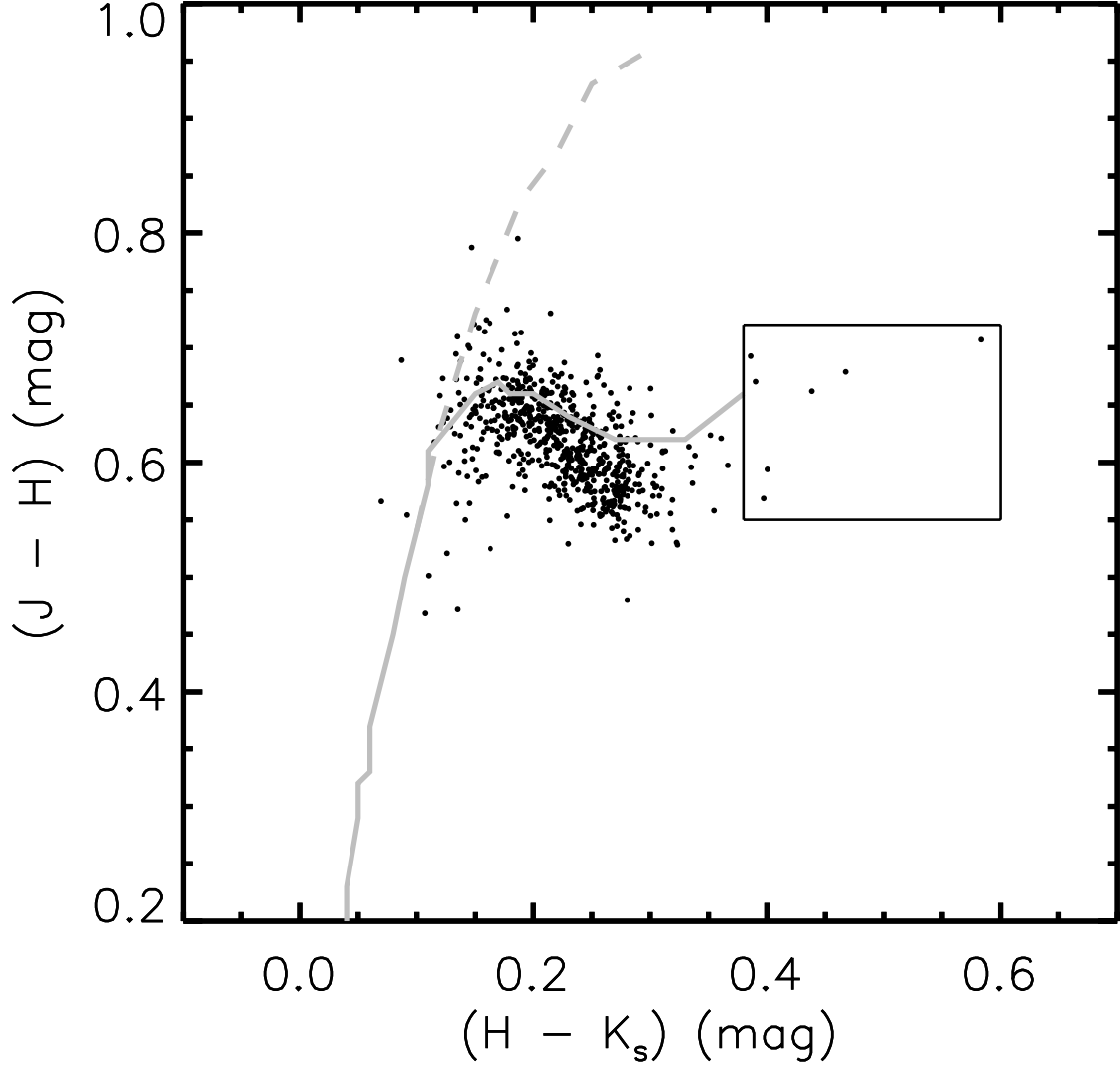


Fig. 7.— Near IR color-color diagram of all candidates (black dots). The expected main sequence (*MS*) dwarf and late-type giant sequences are represented by the solid and dashed gray lines respectively. As expected from the $(V - K_s)$ selection cut, the vast majority of stars in the sample are late-type dwarfs. Several outliers that appear to be giants or earlier-type dwarfs are removed from the sample. The 7 candidates in the solid box have $(H - K_s)$ colors redder than *MS* dwarfs, they are the ultracool candidates discussed in §6

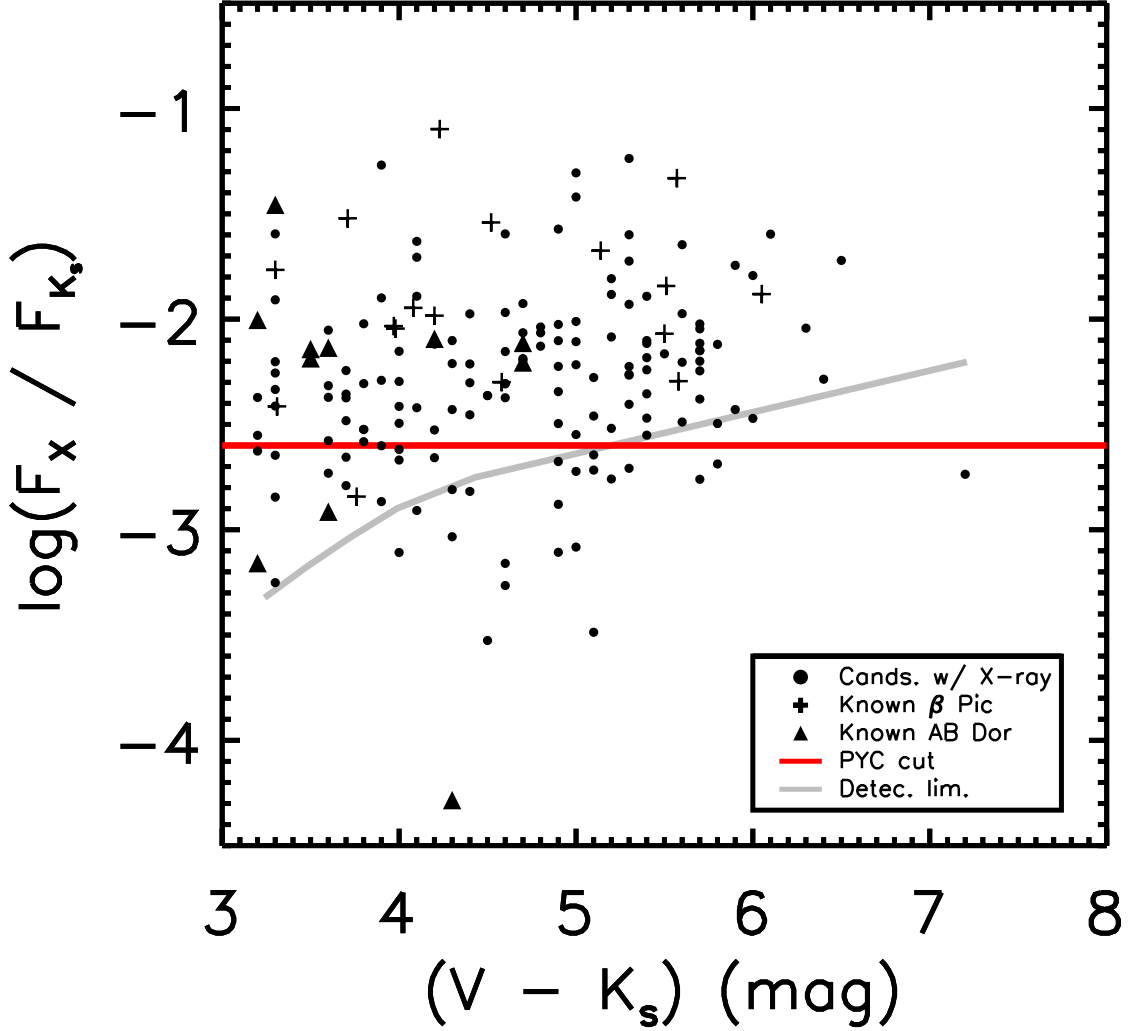


Fig. 8.— X-ray flux ratios for candidates with counterparts in the *ROSAT* catalogs. Known late-type β Pic and AB Dor members are plotted as crosses and upward triangles respectively. Candidates with detected X-ray flux are represented with filled black circles. Candidates lying above the red line at $\log(F_X/F_{K_s}) = -2.6$ have flux ratios consistent with youth as described in the text. These stars are kept in the probable young candidate (*PYC*) sample. Candidates falling below this line are removed. Known AB Dor member BD+01 2477 has a flux ratio well below the cut (~ -4.3) and should be investigated further. The gray line is the estimated X-ray detection limit described in the text. A color version of this figure is available in the electronic journal.

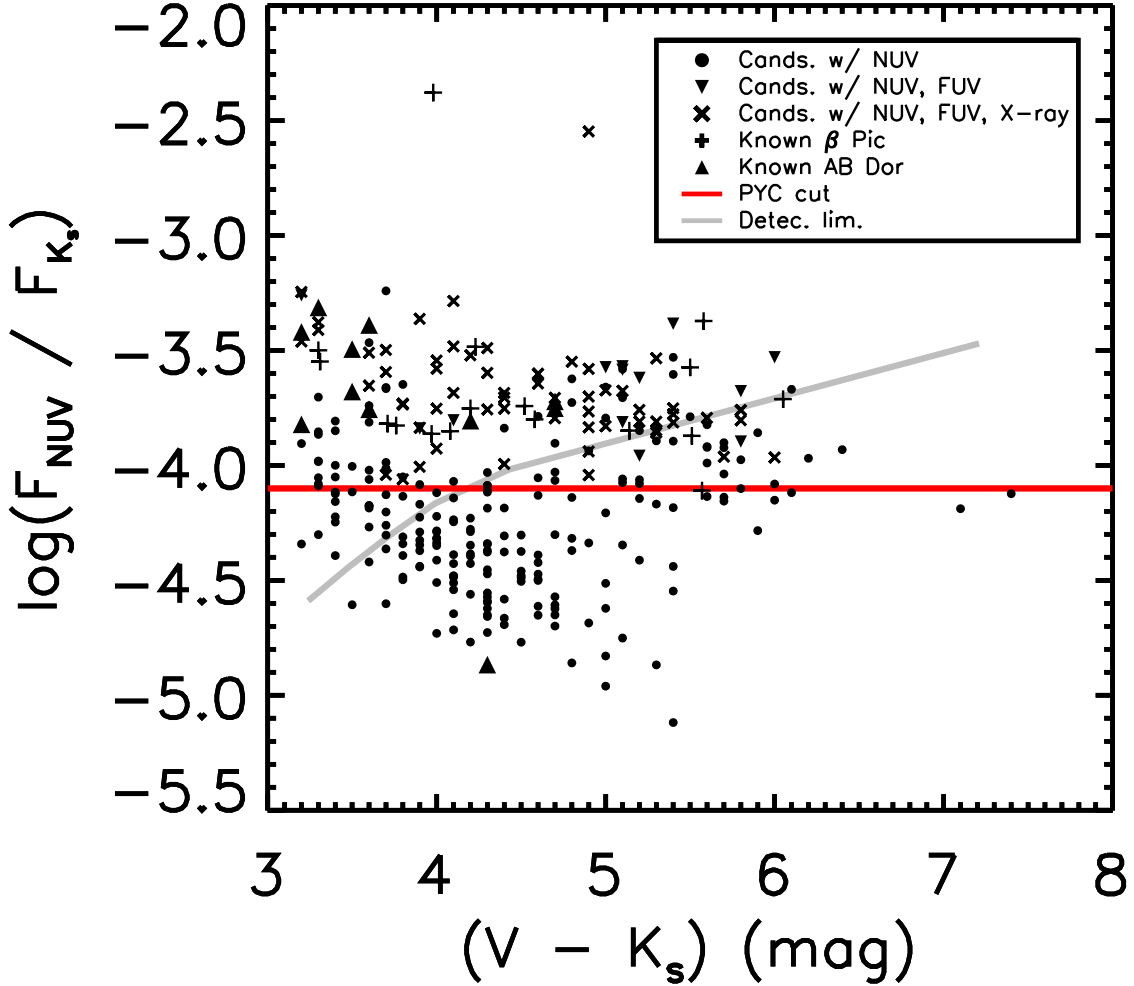


Fig. 9.— *NUV* flux ratios for candidates with counterparts in *GALEX*. Known *NYMG* symbols are identical to Fig. 8. Candidates having only *NUV* flux detections are represented by filled black circles. The red line at $\log(F_{\text{NUV}}/F_{K_s}) = -4.1$ represents the cut imposed for youth in the text. Candidates lying above this line are considered young and are kept in the probable young candidate (*PYC*) sample. Candidates falling below this line are removed. Candidates with strong *NUV*, *FUV*, and X-ray are represented with a black X. Downward facing triangles represent candidates with strong *NUV* and *FUV* but no X-ray that would have been missed if only *ROSAT* data were considered. One candidate not plotted was mostly likely observed during a flare and has *NUV* and *FUV* flux ratios -1.34 and -1.29 respectively. BD+01 2477, a member of the AB Dor group, again has flux well below the youth cut (~ -4.8 , see also R11). The gray line is the estimated *NUV* detection limit described in the text. A color version of this figure is available in the electronic journal.

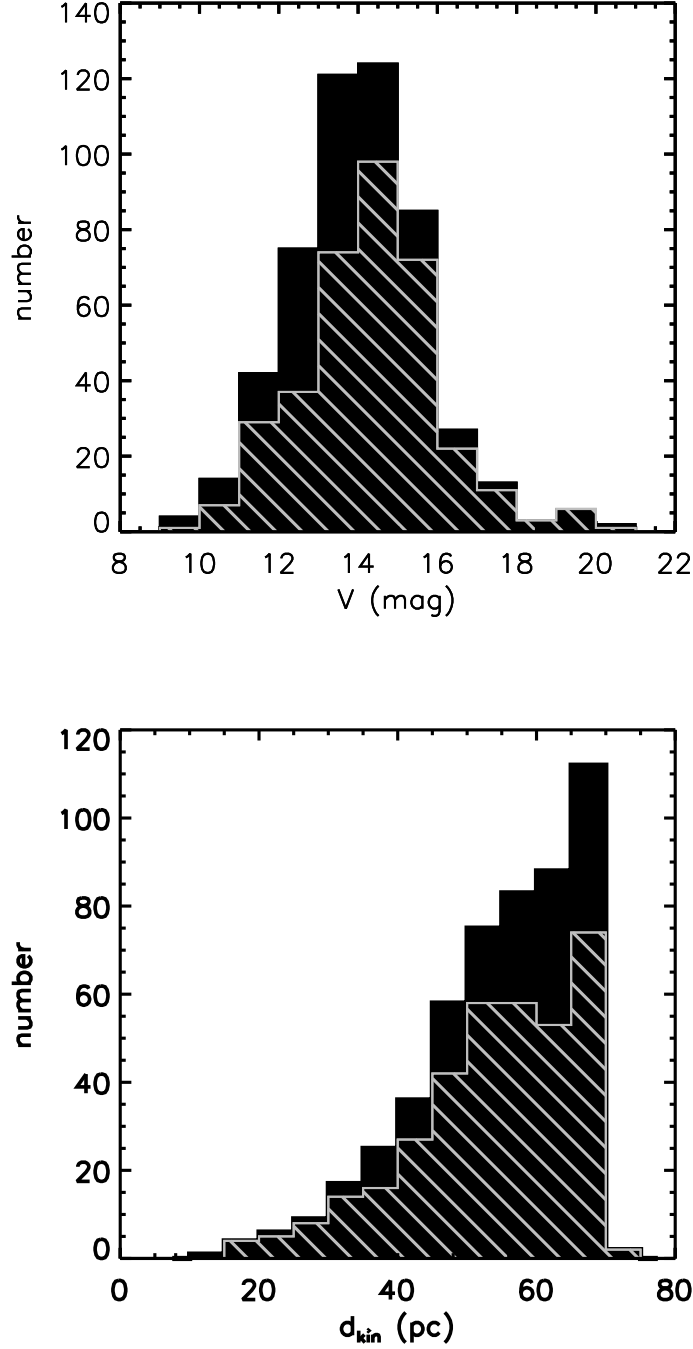


Fig. 10.— V (top) and d_{kin} (bottom) distributions for candidates undetected (UCs) by *ROSAT* (solid, black) and *GALEX* (hashed, gray). The majority of UCs have $V \sim 13-15$ and $d_{kin} \gtrsim 50$ pc. This is consistent with most UCs being true main-sequence interlopers with increasing numbers as search volume increases. Fewer candidates are undetected by *GALEX* since it is more sensitive than *ROSAT*. The sensitivity advantage of *GALEX* is also apparent in the shift of the V distribution to fainter magnitudes and in the approximate flattening of the d_{kin} distribution after 50 pc.

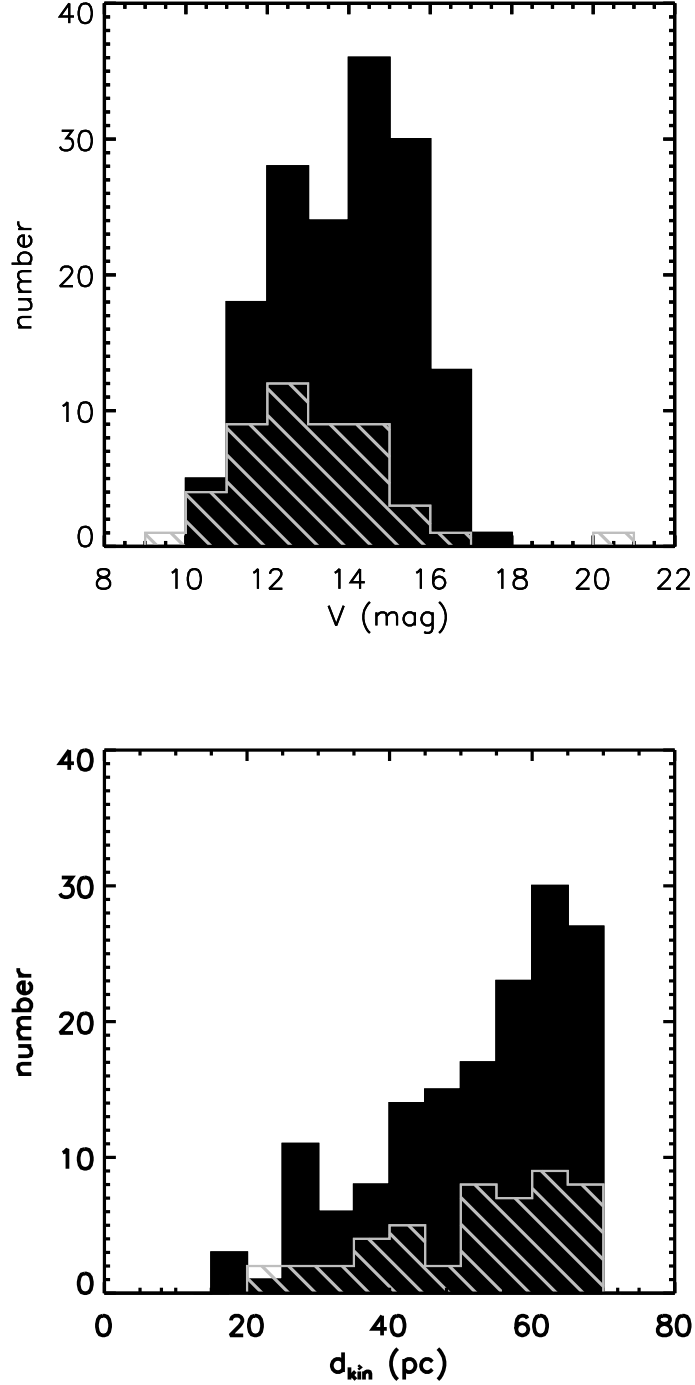


Fig. 11.— Northern probable young candidate (*PYC*) V mag (top) and d_{kin} (bottom) distributions. *BPMG* (hashed, gray) and *ABDMG* (solid, black) histograms exhibit differences in both distributions. *BPMG* candidates are brighter on average and there are fewer at large predicted distances. Because of its older age, the *ABDMG* suffers from greater contamination as search volume increases. The distributions indicate that *BPMG* candidates are more promising targets for follow up and may yield a higher success rate.

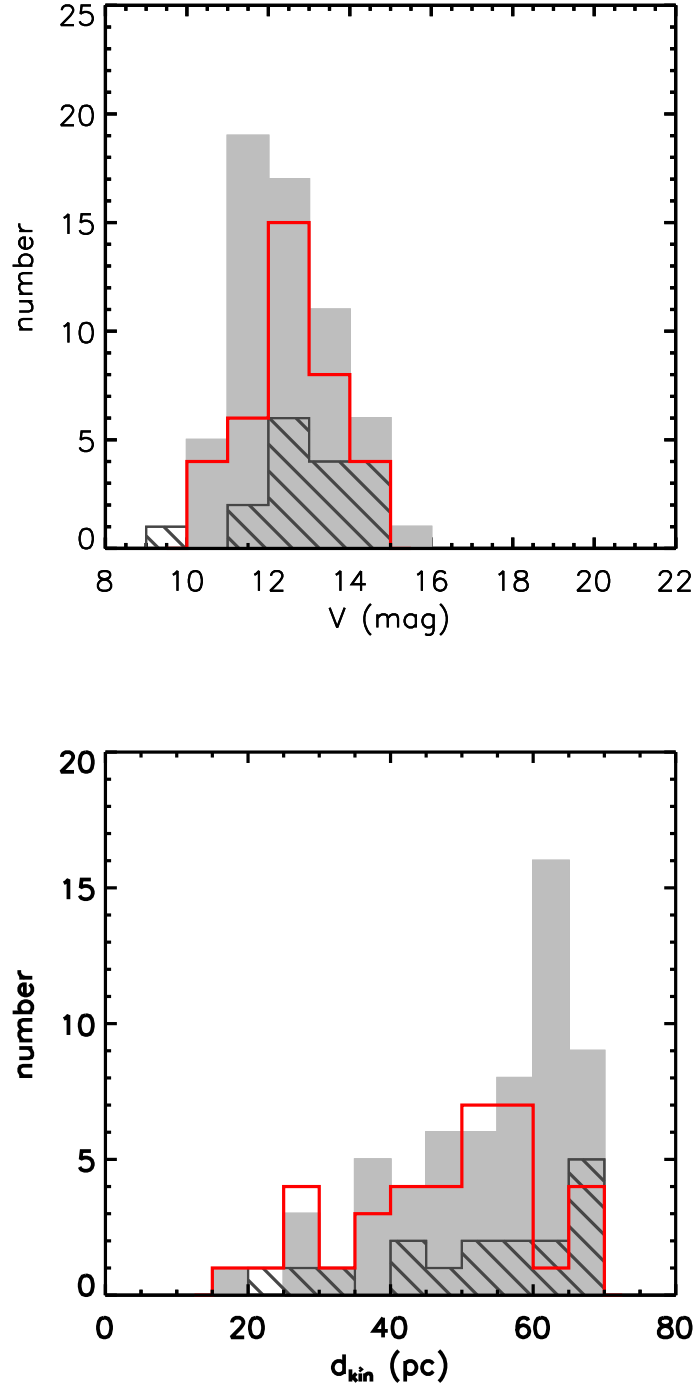


Fig. 12.— Candidates with reliable youth (*CWRV*) activity index (A) V mag (top) and d_{kin} (bottom) distributions. Histograms represent *CWRVs* with $\Sigma A = 1$ (solid, gray), 2 (hashed, dark gray), and 3 (open, red). Many of the *CWRVs* are candidates having only one strong activity indicator; typically only strong X-ray or *NUV*. There are more *CWRVs* with $\Sigma A = 3$, those with the strongest indication of youthful activity, than $\Sigma A = 2$. The $\Sigma A = 3$ distance distribution also peaks at smaller d_{kin} . This combination of multiple strong activity indicators, relatively bright V mags, and smaller predicted distances makes these candidates high priority for follow up investigations. A color version of this figure is available in the electronic journal.

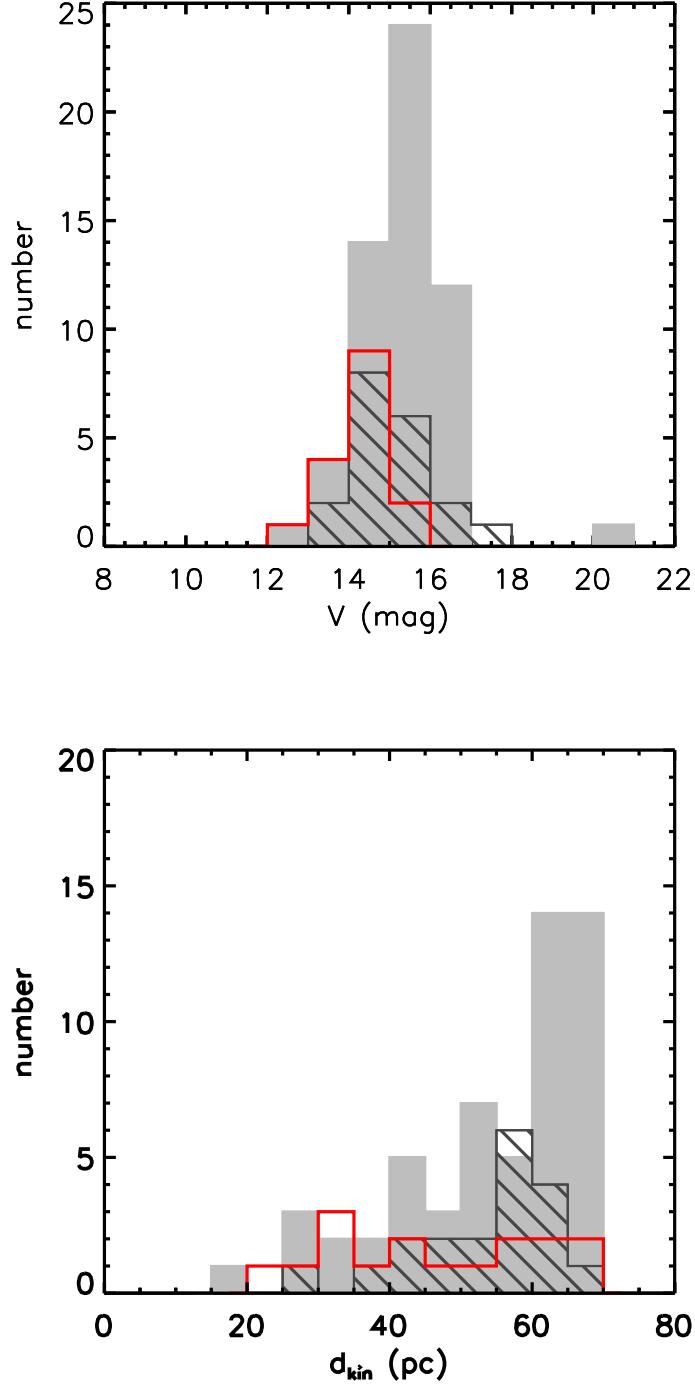


Fig. 13.— Candidates with ambiguous youth (*CWAY*) activity index (A) V mag (top) and d_{kin} (bottom) distributions. The three histograms represent *CWAY*s with the same cumulative A values described in Fig. 12. Because *CWAY*s are candidates with redder ($V-K_s$) colors the V mag distributions are systematically shifted to fainter magnitudes. The d_{kin} distribution of the $\Sigma A = 3$ *CWAY* subsample is approximately flat. This feature is indication that contamination does not increase as volume increases in this subsample. Thus these candidates are prime for follow up. A color version of this figure is available in the electronic journal.

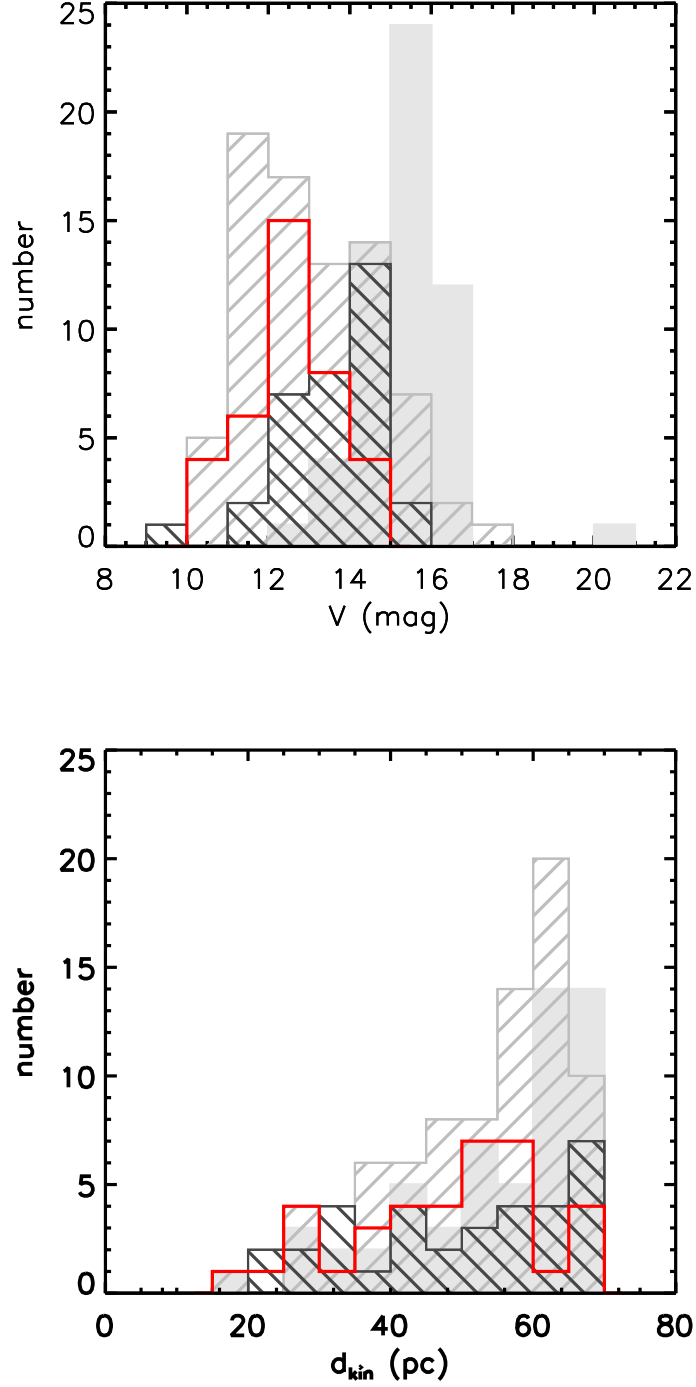


Fig. 14.— Probable young candidate (*PYC*) priority index (*P*) *V* mag (top) and d_{kin} (bottom) distributions. Histograms represent candidates with $P = 1$ (solid, gray), 2 (hashed, light gray), 3 (hashed, dark gray), and 4 (open, red). Candidates with $P = 4$ exhibit many, reliable, strong activity indicators and are the highest priority for follow up. Follow up priority decreases with *P* index. A color version of this figure is available in the electronic journal.

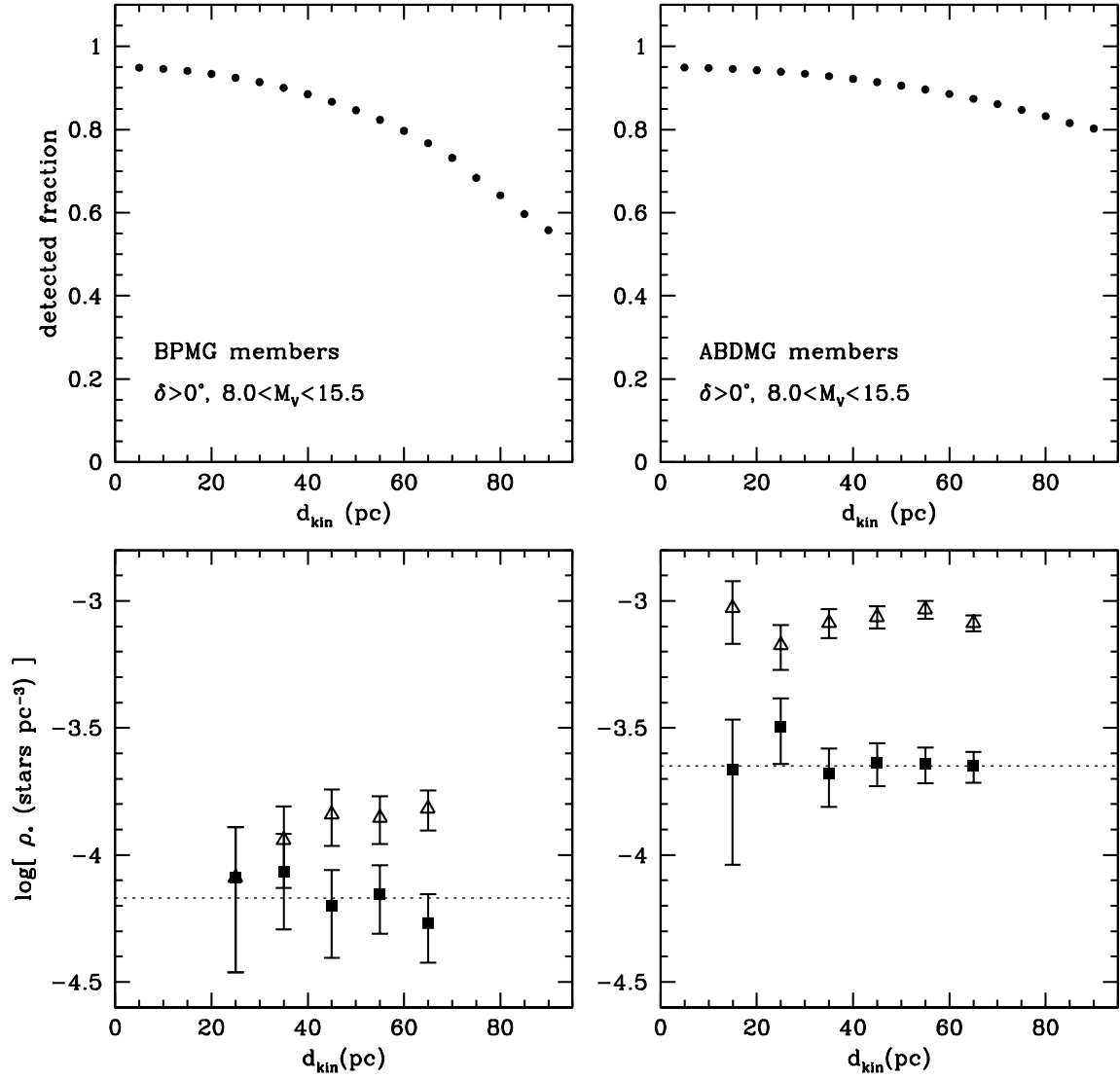


Fig. 15.— Estimated completeness of the search and predicted number densities of northern, low-mass stars in each of the β Pic and AB Dor moving groups. Upper panels: expected rate of detection for stars with absolute magnitudes $8.0 < M_V < 15.5$, typical for young M dwarfs. The main source of incompleteness comes from the proper motion limit ($\mu > 40$ mas yr $^{-1}$) of the source catalog; the incompleteness increases with distance. Lower-panels: volume densities of β Pic (left) and AB Dor (right) moving group candidates, corrected for incompleteness. Estimates based on the full candidate list (open triangles) are compared to estimates using only probable young candidates with strong activity (*PYCs*, filled squares). The latter provide an upper limit estimate for the density of the group in the surveyed volume.